



Article

DUBing Primary Tumors of the Central Nervous System: Regulatory Roles of Deubiquitinases

Thomas Klonisch ^{1,2,3,4} , Susan E. Logue ^{1,4}, Sabine Hombach-Klonisch ^{1,2}  and Jerry Vriend ^{1,*}

¹ Department of Human Anatomy and Cell Science, Rady Faculty of Health Sciences, Max Rady College of Medicine, University of Manitoba, Winnipeg, MB R3E 0J9, Canada

² Department of Pathology, Rady Faculty of Health Sciences, Max Rady College of Medicine, University of Manitoba, Winnipeg, MB R3E 0J9, Canada

³ Department of Medical Microbiology & Infectious Diseases, Rady Faculty of Health Sciences, Max Rady College of Medicine, University of Manitoba, Winnipeg, MB R3E 0J9, Canada

⁴ CancerCare Research Institute, CancerCare Manitoba, Winnipeg, MB R3E 0J9, Canada

* Correspondence: jerry.vriend@umanitoba.ca

Abstract: The ubiquitin proteasome system (UPS) utilizes an orchestrated enzymatic cascade of E1, E2, and E3 ligases to add single or multiple ubiquitin-like molecules as post-translational modification (PTM) to proteins. Ubiquitination can alter protein functions and/or mark ubiquitinated proteins for proteasomal degradation but deubiquitinases (DUBs) can reverse protein ubiquitination. While the importance of DUBs as regulatory factors in the UPS is undisputed, many questions remain on DUB selectivity for protein targeting, their mechanism of action, and the impact of DUBs on the regulation of diverse biological processes. Furthermore, little is known about the expression and role of DUBs in tumors of the human central nervous system (CNS). In this comprehensive review, we have used publicly available transcriptional datasets to determine the gene expression profiles of 99 deubiquitinases (DUBs) from five major DUB families in seven primary pediatric and adult CNS tumor entities. Our analysis identified selected DUBs as potential new functional players and biomarkers with prognostic value in specific subtypes of primary CNS tumors. Collectively, our analysis highlights an emerging role for DUBs in regulating CNS tumor cell biology and offers a rationale for future therapeutic targeting of DUBs in CNS tumors.

Keywords: brain tumor; glioma; neuronal system tumor; deubiquitinase (DUB); endoplasmic reticulum associated degradation (ERAD); immune response; therapeutic target; DNA repair



Citation: Klonisch, T.; Logue, S.E.; Hombach-Klonisch, S.; Vriend, J. DUBing Primary Tumors of the Central Nervous System: Regulatory Roles of Deubiquitinases.

Biomolecules **2023**, *13*, 1503. <https://doi.org/10.3390/biom13101503>

Academic Editors: Qingping Dou and Xin Chen

Received: 7 September 2023

Revised: 4 October 2023

Accepted: 7 October 2023

Published: 10 October 2023



Copyright: © 2023 by the authors. Licensee MDPI, Basel, Switzerland. This article is an open access article distributed under the terms and conditions of the Creative Commons Attribution (CC BY) license (<https://creativecommons.org/licenses/by/4.0/>).

1. Introduction

The ubiquitin proteasome system (UPS) is a highly regulated and dynamic process that utilizes a three-step enzymatic cascade to attach small molecules of the ubiquitin family onto proteins to alter their function and/or mark ubiquitinated proteins for proteasomal degradation. The extensive Ubiquitin and Ubiquitin-like Conjugation Database (UUCD) lists enzymes involved in ubiquitin post-translational modification of proteins [1]. In eukaryotes, this includes 1 human ubiquitin-activating (E1) enzyme (although the literature recognized at least two E1 enzymes, UBA1 and UBA6), 43 E2 ubiquitin-conjugating enzymes, 468 enzymes with E3 ligase activity (further classified as those with RING, HECT, or UBR domains), 538 E3 ligase adaptors, and approx. 100 deubiquitinase enzymes (DUBs) [2,3]. Ubiquitin is one of several ubiquitin-like protein modifiers that also includes ubiquilins, SUMO, NEDD8, and ISG15 [4]. While cellular regulators in their own right, these post-translational modifiers can cross-communicate with ubiquitin through modifications or are being modified by (poly)ubiquitin [5]. Ubiquitin has eight ubiquitination sites, including seven lysine (K) residues (K6, K11, K27, K29, K33, K48, K63) and a primary amine at the N-terminus [5]. While mono-ubiquitination and K48- and K63-linked polyubiquitination are the most abundant forms, multiple other types of ubiquitination exist which have

distinct functional outcomes [6]. Mono-ubiquitination refers to the attachment of a single ubiquitin molecule to a target protein and serves as a signal for protein recognition, complex formation, or allosteric regulation. The addition of a single ubiquitin moiety during mono-ubiquitination can influence the localization, activity, or interaction of the modified protein within the cell. Poly-ubiquitination refers to the formation of a covalently linked ubiquitin molecule chain attached to a specific lysine residue of ubiquitin. When a protein is poly-ubiquitinated with K48-linked ubiquitin chains, it is recognized by the proteasome and targeted for degradation. Unlike K48-linked ubiquitin chains, K63-linked ubiquitin chains do not target proteins for degradation but enable context-specific functions of K63 ubiquitinated proteins in cellular signaling, intracellular trafficking, autophagy, and DNA damage responses [7,8]. K63-linked ubiquitin chains serve as scaffolds for protein–protein interactions, modulate enzyme activity, and regulate the localization and function of target proteins [9,10].

Deubiquitinating enzymes (DUBs) contribute to the regulation of a variety of biological processes, including proteasomal degradation of proteins, cell cycle regulation, histone modifications, transcriptional and translational control, protein trafficking, macro- and mitophagy, DNA damage response, epigenetic processes, and immune response signaling [5]. DUBs reverse the process of protein ubiquitination by selectively removing ubiquitin molecules or chains from proteins. Hence, DUBs are editors of the ubiquitin code and remove single ubiquitin molecules, entire ubiquitin chains, or ubiquitin branches from a ubiquitinated protein by cleaving ubiquitin substrate bonds and ubiquitin–ubiquitin peptide bonds [11,12]. The approx. 100 putative DUBs identified so far in the human proteome are classified into five major families based on their structural and functional characteristics [13–15]. The ubiquitin-specific proteases (USPs) are the largest subclass of DUBs, with currently 54 members in humans [16]. USPs contain a conserved catalytic domain known as the ubiquitin-specific protease domain and exhibit specificity towards different types of ubiquitin linkages. Ubiquitin carboxy-terminal hydrolases (UCH) family members (four members) possess a distinct catalytic domain called the UCH domain. UCHL members are involved in the processing of ubiquitin precursors and the removal of ubiquitin from proteins [17–19]. DUBs of the ovarian tumor proteases (OTU) family (16 members) contain an ovarian tumor (OTU) domain and are involved in various cellular processes, including immune signaling, pathogen infection, and DNA damage response [20–22]. The Machado–Joseph disease proteases (MJD) family of DUB proteins (four members) possesses a Josephin domain, prefers K48/ K63 linkages, and is associated with neurodegenerative disorders, particularly Machado–Joseph disease [23]. The JAB1/MPN/Mov34 (JAMM) metalloenzyme family (16 members) of DUBs contains a metalloprotease domain and prefers targeting K63 ubiquitination sites. JAMM member CSN5 is a deNEDDylase [24–26]. The MINDY family is a recent DUB addition, with two of the four family members containing a “motif interacting with ubiquitin” (MIU) which assists in the enzymatic cleave of long K48 polyubiquitin chains [27]. Finally, a diverse group of ubiquitin-like proteases (ULPs) targets ubiquitin-like modifiers other than ubiquitin and comprises SENP (sentrin/ SUMO-specific protease), DeSI (deSUMOylating isopeptidase) families], and NEDD8 [28–30].

DUBs are essential for the dynamic and coordinated actions of the UPS and ensure proper functions of virtually all cellular processes, including the control of cellular levels of key regulatory transcription factors, growth factors, morphogens, cell cycle regulators, and the balance of factors regulating cell survival. The enzymatic removal of ubiquitin groups by DUBs is critical for reversible ubiquitination and the recycling of unbound ubiquitin to the UPS and ERAD (endoplasmic reticulum-(ER) associated degradation) pathways. Cellular DUB activity determines the coordinated regulation of both the UPS and ERAD pathways in a tissue region- and context-specific manner [31].

Extending throughout eukaryotic cells, the ER is the largest cellular organelle and composed of a series of sheet-like and tubular structures that form close contacts with other organelles, in particular the nucleus and mitochondria [32]. The ER can be subdivided into two types, the smooth and the rough ER. While the smooth ER facilitates lipid synthesis

and hormone synthesis, the rough ER is the site of protein folding, modification, and quality control [32]. Signal peptides direct newly synthesized proteins to the ER lumen where ER-localized chaperones and enzymes facilitate protein folding and modifications. Correctly folded and processed proteins are then shuttled, via transport vesicles, to the Golgi apparatus and from there to their final destination [33]. The folding and modification of proteins is highly dependent on the maintenance of a stable ER environment. Exposure to stresses, such as oxygen and glucose deprivation or loss of ER calcium lowers protein folding efficiency, resulting in the accumulation of unfolded/misfolded proteins [34]. ER function can also be compromised by protein folding demands exceeding capacity. An example is viral infections where the capacity of the ER to facilitate protein folding is overwhelmed, giving rise to misfolded proteins [35]. Irrespective of the initiating stimulus, the buildup of misfolded/unfolded proteins is commonly referred to as ER stress. Cells combat ER stress by initiating an adaptive, highly conserved stress response referred to as the Unfolded Protein Response or UPR. The UPR is controlled by three ER-anchored transmembrane receptors, Inositol-requiring enzyme 1 (IRE1), protein kinase R (PKR)-like endoplasmic reticulum kinase (PERK), and activating transcription factor 6 (ATF6). These three ER-based receptors monitor ER health. In an unstressed setting, each of these stress sensors is held in an “off” position by binding their luminal domain to the ER chaperone Grp78 (BIP, HSPA5) [36,37]. Upon ER stress, Grp78 dissociates from IRE1, PERK, and ATF6, which stimulates their transition from inactive to active states [36,37]. Downstream signaling pathways orchestrated by IRE1, PERK, and ATF6 function in a co-operative, complementary manner to support the refolding of those proteins that can be refolded. Those proteins beyond repair are removed via the ER-associated degradation or ERAD pathway [34]. Ultimately, the objective of the UPR is to reduce ER stress, thereby restoring ER homeostasis. A functional UPS is a critical element of this cellular quality control system and DUBs are dynamically involved in this process.

Cancer cells frequently endure both external stressors (e.g., hypoxia and glucose deprivation) and internal stresses triggered by their high proliferation and metabolic rate. To thrive under such conditions and escape immune responses, cancer cells engage and coordinate adaptive responses, including UPS, ERAD, UPR, and DNA damage repair [38–41]. Although these responses may initially be engaged to aid cellular stress adaptation, cancer cells usurp and/or co-opt these pathways for their benefit in numerous ways. We recently identified distinct gene expression changes in ubiquitin ligases and ligase adaptors in different human brain tumors and subtypes [42,43]. Sustained UPR signaling has been reported in diverse cancers, including breast, prostate, and brain cancers, and emerging evidence links ERAD and UPR to an array of pro-tumorigenic processes, including angiogenesis, metastasis, and cancer stem cell expansion [38].

DUBs are an integral part of the UPS but their role in human brain tumors is incompletely understood. We gathered that understanding the role of DUBs in brain tumors could yield new therapeutic avenues. In the present study, we have analyzed the gene expression profiles of 99 human DUBs belonging to 7 subgroups listed in the HUGO (Human Genome Organization) classification. The objective of the current study was to comprehensively examine the differential gene expression of these DUBs in publicly available datasets of selected human neuronal system tumors, including pediatric craniopharyngioma (CPh), ependymoma (EPN), medulloblastoma (MB), adult brain tumors (astrocytoma (AS), oligodendroglioma (ODG), glioblastoma (GBM), and neuroblastoma (NBT) tumors arising from the developing sympathetic nervous system as the most common childhood extra-cranial neoplasm [44,45]. Some of the datasets had available gene expression data of non-tumor tissues for comparison, while other datasets had available age data for each subject. This allowed for plotting gene expression by tumor subgroup and by age for each DUB and enabled the comparison of gene expression in pediatric vs adult age groups. Adding novel insight, we sought to determine whether the expression of DUB genes was selective for specific CNS tumors, specific subgroups of CNS tumors, or specific age groups of subjects with these brain tumors. For those datasets with survival data, we determined whether

DUB gene expression was statistically associated with survival. Top DUB hits identified in these bioinformatic screens were interrogated for their association with ERAD, UPR, and DNA repair. This is the first comprehensive report with a focus on DUB family members in selected pediatric and adult brain tumors, their relationship with ERAD, UPR, DNA damage repair pathways, and their suitability as potential biomarkers and therapeutic targets in defined CNS tumors. However, the function of some of the DUBs mentioned in the current report has previously been described in relation to CNS tumorigenesis [46,47].

Microarray datasets of CNS tumors available for the current study included those of glioma, ependymoma, medulloblastoma, craniopharyngioma, and neuroblastoma. Glioma originate from glial cells in the brain and include astrocytoma, glioblastoma, oligodendroglioma, and ependymoma. AS and GBM are considered to originate from astrocytes according to the WHO classification and astrocytoma can convert into GBM [48]. The hypothesis that GBM can originate from neural stem cells has also been proposed [49,50]. ODG originate from oligodendrocytes, while EPN derived from a type of glial cells called ependymocytes can be present intracranially and in the spinal cord, which affects treatment strategies [51,52]. MB are grouped by a consensus classification into four subgroups, the WNT group originating in the lower rhombic lip area of the hindbrain, the SHH group originating in the upper rhombic lip area [53], while MBs in Groups 3 and 4 arise from progenitor cells in the ventricular rhombic lip [54]. In the Cavalli dataset, each of the four consensus groups has been further characterized for subtype-specific molecular and clinical differences. A recent review has summarized the significance of molecular subtypes for the diagnosis and treatment of MB [55]. CPh are non-glial tumors originating in the hypothalamic and pituitary regions and are associated with remnants of Rathke's pouch. Alomari et al. (2015) have presented a case of craniopharyngioma derived from Rathke's cleft cyst and have reviewed the literature supporting the view that CPh originate from Rathke's pouch cells [56]. NBT are sympathetic nervous system tumors originating from neural crest cells [57] and several excellent reviews discuss therapeutic strategies for NBT [58–60].

2. Methods

We utilized the human genome list of 99 deubiquitinases to determine the expression of these DUB genes in publicly available datasets of brain tumors. Differential expression of DUB genes was examined in these datasets made available in the R2 Genomics Analysis and Visualization platform (<https://r2.amc.nl> (accessed on 5 September 2023)). We used the AS, GBM, ODG, and a non-tumor group in the mixed glioma dataset of Sun et al. (Geo ID: GSE4290). Differentially expressed DUB genes were considered significant at $p < 0.001$ as determined by Analysis of Variance (ANOVA) through the R2 Genomics site and plotted using the Morpheus heatmap and cluster analysis program at the Broad Institute website (<https://software.broadinstitute.org/morpheus> (accessed on 5 September 2023)). DUB gene expression of classic, mesenchymal, and proneural GBM subtypes was examined in the TCGA GBM dataset (R2 ID: Tumor Glioblastoma TCGA 540). Survival data associated with differentially expressed DUB genes were examined in the French glioma data (GSE16022) [61]. The Pfister dataset (GSE64415) was used to examine differentially expressed DUB genes in ependymoma. A dataset of Donson (GSE94349) was used to examine the differential expression of DUB genes in CPh, while the datasets of Cavalli et al. [62] (GSE85217) and Weishaupt et al. [63] (GSE124814) were used to examine DUB gene expression in MB subgroups. The Cavalli dataset had extensive data on the age of subjects in the various subgroups, which we used to determine the age distribution for the most highly significant differentially expressed DUB genes. Those DUB genes statistically associated with the survival of MB patients were also determined in the Cavalli dataset. The Weishaupt data (Swartling dataset in the R2 Genomics database) allowed for a comparison of genes between MB tumor tissue and non-tumor tissue. The NBT dataset of Fischer [64] (GSE120572) was used to evaluate various treatment effects on DUB expression. The Cytoscape program was applied to identify gene ontology (GO) pathways, includ-

ing ERAD, DNA repair, immune response pathways, and genes coding for differentially expressed DUBs that were associated with brain tumors.

3. Results

Cytoscape analysis of the 99 DUB genes (GO biological pathways) identified several functional groups of DUBs involved in the deubiquitination of lysine (K) residues K6/K11/K27/K29/K48/K63 ubiquitinated proteins. The most significant biological pathways, other than deubiquitination itself, included DNA repair, DNA methylation, the regulation of ER stress and ERAD pathway, death receptor signaling, and the regulation of immune and cytokine responses.

3.1. Adult Glioma Show Differential Expression of DUBs

In the Sun mixed glioma dataset, the expression of 51 of the 99 DUB genes (HUGO classification) was significantly different ($p < 0.001$) between the 4 groups in the dataset (non-tumor, AS, GBM, ODG). The heatmap (Figure 1) shows the gene expression profiles of the four groups. Table 1 shows the DUB genes that were most significantly different between the non-tumor group and each of the other three adult glioma groups. Seventeen of the ninety-nine DUB genes were differentially expressed ($p < 0.001$) between AS, ODG, and GBM (*USP46*, *USP54*, *ZRANB1*, *USP1*, *OTUD7A*, *TNFAIP3*, *USP27x*, *USP30*, *EIF3H*, *USP49*, *OTUD1*, *USP11*, *OTUB1*, *CYLD*, *USP12*, *USP2*, *USP47*, in order of p value as determined by ANOVA).

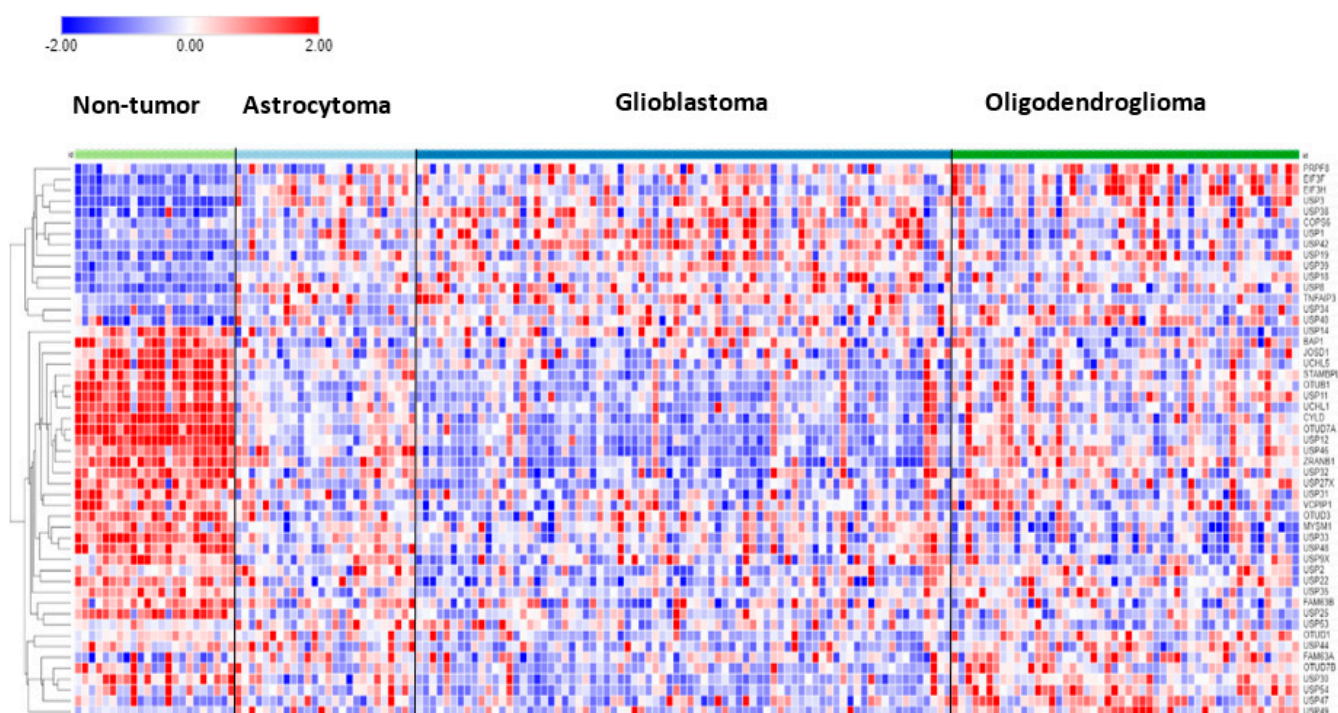


Figure 1. Heatmap and cluster analysis of differentially expressed DUBs in gliomas. Non-tumor, N = 23; Astrocytoma, N = 26; Glioblastoma, N = 77; Oligodendroglioma, N = 50.

Table 1. Top ten differentially expressed DUB genes in gliomas by group compared to non-tumor group.

Astrocytoma ¹	DUB	<i>p</i> Value (Corrected)	Chromosome	Versus Non-Tumor Group in the Sun Dataset
<i>CYLD</i>	Usp	2.44×10^{-13}	16	Down
<i>USP12</i>	Usp	3.73×10^{-12}	13	Down
<i>USP3</i>	Usp	1.95×10^{-11}	15	Up
<i>OTUD7A</i>	Otu	1.26×10^{-10}	15	Down
<i>OTUB1</i>	Otu	4.38×10^{-10}	11	Down
<i>USP8</i>	Usp	1.69×10^{-09}	15	Up
<i>USP33</i>	Usp	8.97×10^{-09}	1	Down
<i>STAMBPL1</i>	Jamm	5.64×10^{-08}	10	Down
<i>EIF3F</i>	Jamm	5.94×10^{-08}	11	Up
<i>EIF3H</i>	Jamm	4.60×10^{-07}	8	Up
Glioblastoma ²				
<i>USP12</i>	Usp	5.22×10^{-20}	13	Down
<i>OTUD7A</i>	Otu	1.13×10^{-19}	15	Down
<i>ZRANB1</i>	Otu	2.37×10^{-18}	10	Down
<i>USP46</i>	Usp	3.60×10^{-18}	4	Down
<i>OTUB1</i>	Otu	4.24×10^{-18}	11	Down
<i>CYLD</i>	Usp	2.34×10^{-16}	16	Down
<i>USP3</i>	Usp	1.20×10^{-13}	15	Up
<i>USP27X</i>	Usp	5.35×10^{-12}	X	Down
<i>USP30</i>	Usp	9.20×10^{-12}	12	Down
<i>USP11</i>	Usp	1.39×10^{-11}	X	Down
Oligodendroglioma ³				
<i>USP12</i>	Usp	3.27×10^{-11}	13	Down
<i>OTUD7A</i>	Otu	3.55×10^{-10}	15	Down
<i>USP48</i>	Usp	6.67×10^{-09}	1	Down
<i>USP33</i>	Usp	1.37×10^{-08}	1	Down
<i>CYLD</i>	Usp	1.45×10^{-08}	16	Down
<i>USP3</i>	Usp	1.50×10^{-08}	15	Up
<i>EIF3F</i>	Jamm	1.57×10^{-08}	11	Up
<i>OTUD3</i>	Otu	2.46×10^{-08}	1	Down
<i>USP14</i>	Usp	4.85×10^{-08}	18	Down
<i>OTUB1</i>	Otu	6.68×10^{-08}	11	Down

¹ Total of 24 DUBs different from NT at $p < 0.0001$; ² total of 43 DUBs different from NT at $p < 0.0001$; ³ total of 30 DUBs different from NT at $p < 0.0001$.

Next, we asked whether the differences in DUB gene expression between AS and GBM were related to the progression from AS to GBM [48], which is associated with several changes in the transcriptome [65]. ANOVA showed that the expression of two DUB genes, *USP46* and *ZRANB1*, differed at a high level of significance ($p < 0.001$) between the AS and GBM groups (Figure 2). *USP46* was among the top 100 of all differentially expressed genes

between the AS and GBM groups in the Sun mixed glioma dataset. Of all 18,896 genes in the French dataset, *ZRANB1* and *USP46* expression were ranked 3rd and 2725th, respectively, when associated with survival. *ZRANB1* belongs to the OTU class of DUBs and has been reported as an EZH2 (enhancer of zeste homolog 2) DUB [66]. EZH2 inhibitors are currently tested for cancer therapy and brain permeable derivatives may offer new avenues in the treatment of brain tumors [67,68].

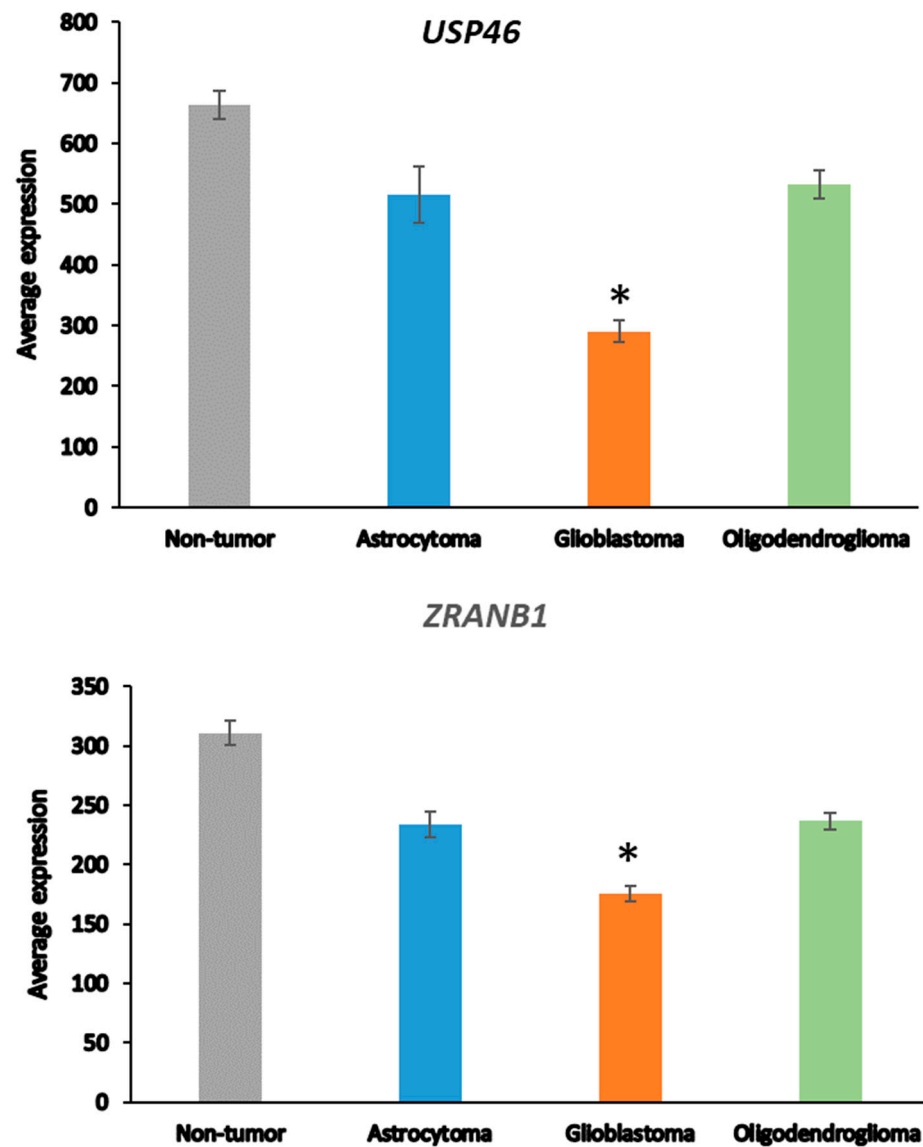


Figure 2. Differential expression of *USP46* and *ZRANB1* in adult glioma groups. *USP46* ($F = 42.34$, $p = 1.53 \times 10^{-20}$); *ZRANB1* ($F = 45.17$, $p = 1.40 \times 10^{-21}$) in the Sun dataset; Non-tumor $N = 23$, Astrocytoma, $N = 26$, Glioblastoma, $N = 77$, Oligodendroglioma, $N = 50$). * indicates significant difference between GBM and AS, $p < 0.0001$.

3.2. Chromosome 10 and DUB Expression in Astrocytic glioma

Table 2 shows DUB gene expression related to survival in the French dataset of glioma subjects. Expression of *ZRANB1*, a gene located on chromosome 10, showed the most significant differences in Kaplan Meier survival curves. In addition to *ZRANB1*, several other differentially expressed DUB genes are also located on chromosome 10. The HUGO list of DUB genes includes two DUBs located on the p arm of chromosome 10 (*OTUD1* and *MINDY3/FAM188A*) and three DUBs that are located on the q arm of chromosome 10

(*ZRANB1*, *USP54*, and *STAMBPL1*). Expression of *ZRANB1* and *USP54* was decreased in the GBM group compared to the AS and non-tumor groups.

Table 2. DUB gene expression and survival data of glioma patients (French dataset).

DUB Gene	Family	Chromosome	Chi Square Kaplan Meier	p Value	Hazard Ratio (HR)	HR p Value	Better Survival
<i>ZRANB1</i>	Otu	10	116.69	3.36×10^{-27}	0.21	4.6×10^{-27}	High
<i>FAM188A</i>	Mindy	10	68.95	1.01×10^{-16}	0.53	1.4×10^{-13}	High
<i>USP34</i>	Usp	2	63.01	2.06×10^{-15}	0.30	4.4×10^{-12}	High
<i>USP49</i>	Usp	6	63.46	1.63×10^{-15}	0.55	1.9×10^{-16}	High
<i>Usp27X</i>	Usp	X	57.58	3.24×10^{-14}	0.43	1.6×10^{-15}	High
<i>USP54</i>	Usp	10	51.46	7.30×10^{-13}	0.68	2.5×10^{-11}	High
<i>USP51</i>	Usp	X	49.10	2.43×10^{-12}	0.69	1.4×10^{-11}	High
<i>USP30</i>	Usp	12	43.77	3.69×10^{-11}	0.47	1.5×10^{-8}	High
<i>USP11</i>	Usp	X	42.18	8.33×10^{-11}	0.52	2.6×10^{-10}	High
<i>OTUD7A</i>	Otu	15	38.15	6.54×10^{-10}	0.69	1.3×10^{-9}	High
<i>EIF3H</i>	Jamm	8	35.16	3.40×10^{-9}	0.47	7.1×10^{-10}	High
<i>USP1</i>	Usp	1	33.71	6.39×10^{-9}	1.8	1.4×10^{-8}	Low
<i>USP4</i>	Usp	3	33.07	8.90×10^{-9}	2.6	5.6×10^{-8}	Low
<i>ATXN3</i>	MJD	14	33.10	8.75×10^{-9}	0.65	7.7×10^{-6}	High
<i>USP43</i>	Usp	17	31.76	1.74×10^{-8}	0.74	1.1×10^{-8}	High
<i>USP46</i>	Usp	4	31.45	2.05×10^{-8}	0.65	9.2×10^{-8}	High
<i>TNFAIP3</i>	Otu	6	30.86	2.77×10^{-8}	1.3	6.0×10^{-7}	Low
<i>OTUD1</i>	Otu	10	28.27	1.06×10^{-7}	0.54	2.0×10^{-8}	High
<i>JOSD2</i>	MJD	19	25.88	3.62×10^{-7}	1.5	2.1×10^{-4}	Low
<i>PSMD7</i>	Jamm	16	24.22	8.60×10^{-7}	1.9	1.3×10^{-4}	Low
<i>STAMBPL1</i>	Jamm	10	23.87	1.03×10^{-6}	0.76	4.3×10^{-5}	High
<i>USP14</i>	Usp	18	23.95	9.90×10^{-7}	2.1	1.0×10^{-4}	low

The loss of chromosome 10 in primary GBM or loss of the q arm of chromosome 10 in secondary GBM is a common finding [69,70]. This has led to the hypothesis that the loss of one or more tumor suppressor genes on the q arm of chromosome 10 may contribute to GBM development. The most significant differentially expressed pathway between the AS and GBM group in the Sun dataset was the “*D-glutamine and D-glutamate*” pathway, which was represented by differential expression of two genes, *GLUD1* and *GLUD2* (glutamate dehydrogenase 1 and 2). *GLUD1* is located on chromosome 10 and codes for the mitochondrial matrix enzyme glutamate dehydrogenase 1. *GLUD1* and *GLUD2* expression was lowered to 52.7% and 52.2% compared to the NT and AS groups, respectively. While a role for specific DUBs in the regulation of *GLUD1* has not been established, among all 99 DUB genes we observed the highest correlations of *GLUD1* expression with *USP46* ($r = 0.74$, $p = 1.74 \times 10^{-30}$) and *ZRANB1* ($r = 0.70$, $p = 1.01 \times 10^{-26}$). This suggests a possible new role for *USP46* and/or *ZRANB1* in regulating *GLUD1* in astrocytic glioma (AS and GBM).

3.3. Differential Expression of DUBs in GBM Subtypes

The differential expression of DUB genes was determined in three GBM subtypes from a TCGA dataset in the R2 genomics platform. *TNFAIP3* showed the most significant difference ($p = 7.68 \times 10^{-09}$) with elevated expression in the mesenchymal GBM subtype (Figure 3). The DUBs with the most significantly elevated gene expression in the proneural GBM group were *USP11*, *USP22*, and *USP7*.

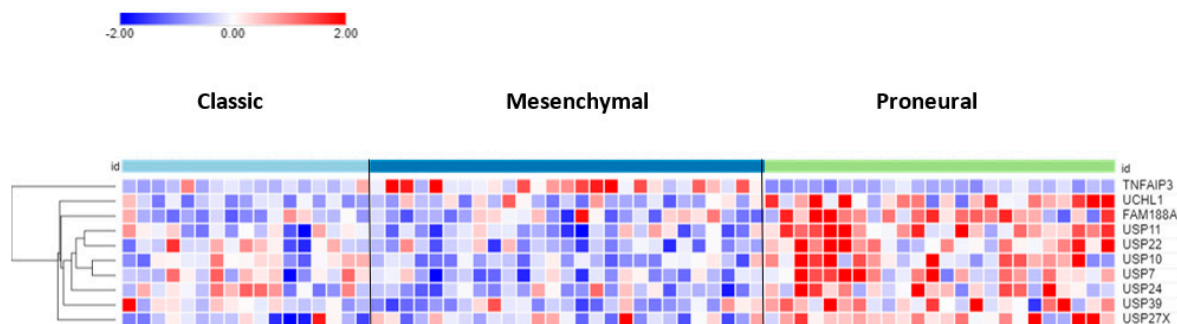


Figure 3. Heatmap and cluster analysis of DUB genes differentially expressed in GBM subtypes. On average, *TNFAIP3* expression was higher in the GBM mesenchymal group, whereas the expression of the other 9 genes was higher in the proneural group. Classic, N = 17; Mesenchymal, N = 27; Proneural, N = 24).

3.4. Relationship between DUB Expression and Survival (French Dataset)

Survival data were not available in the Sun mixed glioma dataset. Hence, we used the glioma dataset (GSE16011) of French et al. [61] (N = 284) to determine survival data associated with DUB gene expression. Kaplan Meier curves showed that the expression of 23 DUB genes was significantly associated ($p < 0.001$) with survival in glioma patients. Table 2 lists the Chi square, p values, and hazard ratios for these DUB genes. The most significantly downregulated DUB gene, *ZRANB1* (as would be expected with loss of chromosome 10 or its q arm), was associated with worse survival (Table 2).

3.5. Role of DUBs in ER Stress and ERAD Signaling in Glioma

Employing the R2 genomics platform to query the 99 DUBs for their association with the GO category of *Regulation of the ERAD pathway*, we identified 3 DUB genes in this category as differentially expressed in the glioma dataset: *USP14*, *USP19*, and *USP25* (Table 3). It should be noted, however, that only *USP14* was among the most significant in Table 1. In the French dataset, high *USP14* expression was associated with worse survival (Table 2). The role of *USP14* and *USP19* proteins in ER stress has been illustrated in a review by Qu et al. [31]. *USP19* is reported to inhibit the unfolded protein response [71] and to deubiquitinate the E3 ligase *HRD1* [72], a component of the ERAD pathway. *USP14* binds to *IRE1* and is reported to be an inhibitor of the ERAD pathway [73]. *USP25* deubiquitinates selected ERAD substrates [74]. Another DUB reported by Qu et al. to regulate ER stress-induced apoptosis is *BAP1* [31]. Differential *BAP1* gene expression is also shown in Table 3.

Table 3. Differential expression of DUBs in ERAD signaling in glioma.

DUB Gene	Non-Tumor N = 23	Astrocytoma N = 26	Glioblastoma N = 77	Oligodendroglioma N = 50
<i>USP14</i>	851.87 ± 25.31	689.66 ± 25.63 *	738.5 ± 18.13 *	647.71 ± 16.28 *
<i>USP19</i>	159.11 ± 6.47	206.93 ± 9.5 *	222.11 ± 6.09 *	226.03 ± 7.9 *
<i>USP25</i>	314.57 ± 14.19	216.77 ± 9.34 *	216.88 ± 9.18 *	209.77 ± 7.59 *
<i>BAP1</i>	295.14 ± 10.78	221.5 ± 7.97 *	244.66 ± 5.02 *	248.25 ± 6.88 *

USP14 (F = 12.27, $p = 2.58 \times 10^{-07}$), *USP19* (F = 10.53, $p = 2.16 \times 10^{-06}$), *USP25* (F = 14.59, $p = 1.64 \times 10^{-08}$), *BAP1* (F = 11.06, $p = 1.12 \times 10^{-06}$). * Significantly different from non-tumor group at $p < 0.001$.

3.6. DUBs in the Regulation of Immune Responses in Glioma

Among the 99 DUB genes, 4 differentially expressed genes were identified in the Sun glioma dataset that were associated with the GO category of *Regulation of the immune response*. This included *OTUD7A*, $F = 69.909$, $p = 1.31 \times 10^{-29}$, *CYLD*, $F = 50.614$, $p = 1.69 \times 10^{-23}$, *TNFAIP3*, $F = 11.84$, $p = 4.34 \times 10^{-07}$, and *USP18*, $F = 8.14$, $p = 4.21 \times 10^{-05}$ (Figure 4). Notably, the expression of *OTUD7A* was not only the most significantly different among the DUBs in the GO category of *Regulation of immune response* but was also the most significant of any of the 512 genes in this category in the Sun dataset. *OTUD7A* expression was significantly decreased in AS, GBM, and ODG (Figure 4), as was *OTUB1* in all three types of gliomas compared to non-tumor tissues in the Sun dataset (Table 1). *OTUB1* deubiquitinase function was recently associated with the regulation of immune responses and contributes to immunosuppression in cancers via the programmed death ligand 1 (PD-L1) protein [75]. Decreased *OTUB7A* and *OTUB1* gene expression may both affect immune responses and DNA damage repair functions (see below) in glioma [75,76].

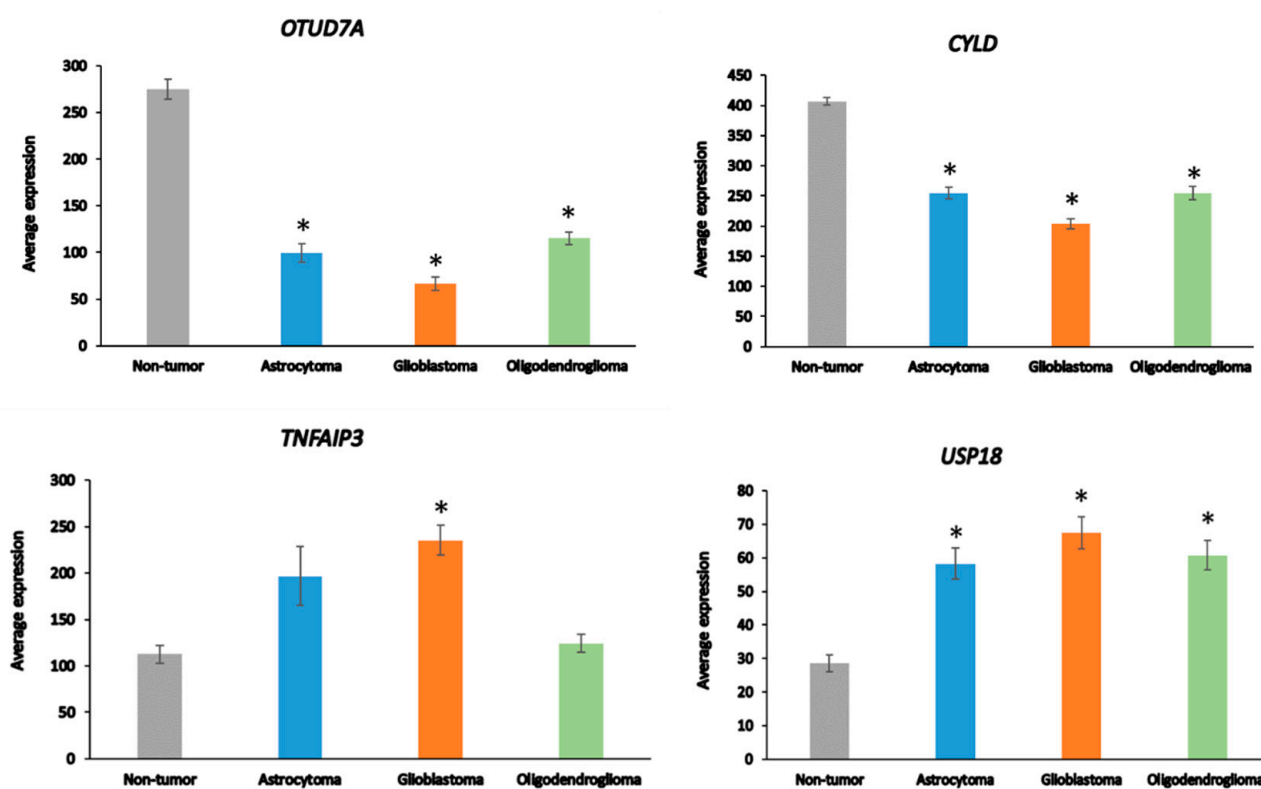


Figure 4. Differentially expressed DUBs identified under the GO category of *Regulation of immune response* in different glioma and non-tumor brain. * $p < 0.001$ compared to non-tumor group.

The *OTUD7A* gene is located on chromosome 15q13.3. Microdeletion of this chromosomal region results in abnormalities of neuronal development [77,78]. *CYLD* is a tumor suppressor that contributes to the regulation of NF- κ B [79]. *TNFAIP3* plays a role in several aspects of the immune response, including the regulation of NF- κ B and the regulation of inflammation [80]. *TNFAIP3* deletions have been associated with Epstein–Barr viral infection in lymphomas [81]. *USP18* regulates interferon signaling by binding to one of its receptors (IFNAR2) [82].

3.7. DUBs and DNA Repair in Glioma

Ten of the ninety-nine DUB genes analyzed in the Sun dataset were differentially expressed genes associated with the GO category of *DNA repair*: *OTUB1*, *UCLH5*, *USP3*, *USP1*, *USP51*, *COPS5*, *COPS6*, *USP10*, *USP47*, and *USP43* (in order of significance in ANOVA). The expression of *OTUB1* and *UCLH5* was significantly decreased ($p < 0.001$)

in AS, GBM, and ODG compared to non-tumor tissue, while the expression of *USP3* was significantly elevated ($p < 0.001$) (Figure 5). Expression of *USP1* was markedly increased in GBM and, to a lesser extent, in AS compared to the non-tumor group. Several DUBs, including *USP1*, *OTUB1*, *UCHL5*, and *USP47*, have been included in a list of 16 DUBs reported to be involved in specific DNA damage repair pathways [83]. *OTUD7A* (Cezanne2) has also recently been reported to contribute to the DNA damage response in double-strand break (DSB) repair [84] and expression of *OTUD7A* was substantially reduced in gliomas compared to non-tumor brain tissue (Figure 4). While linked to several DNA repair pathways [83], *USP7* and *USP24* expression was not significantly different among glioma groups or between glioma and the non-tumor control group in the Sun dataset, suggesting that these two DUBs may not be critical factors in DNA damage repair pathways in glioma.

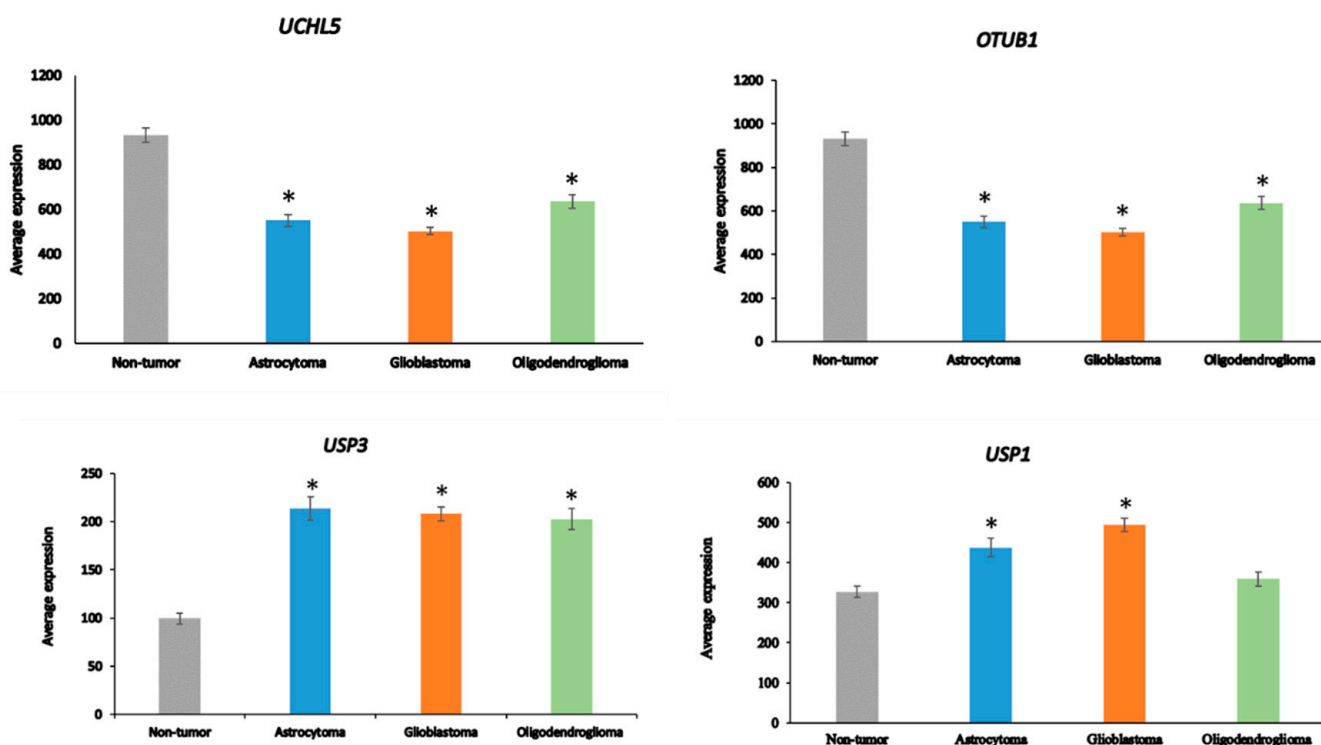


Figure 5. Differentially expressed DUB genes in the GO category of DNA repair. *UCHL5*, $F = 21.83$, $p = 4.97 \times 10^{-12}$; *OTUB1*, $F = 42.71$, $p = 1.12 \times 10^{-20}$; *USP3*, $F = 19.33$, $p = 7.56 \times 10^{-11}$; *USP1*, $F = 16.99$, $p = 1.04 \times 10^{-09}$. * $p < 0.001$ compared to non-tumor group by t-test.

3.8. DUBs in Ependymoma

The heatmap and cluster analysis shown in Figure 6 illustrate clusters of DUB gene expression that differ significantly between the EPN subgroups of the Pfister dataset. Of all molecular subgroups in this dataset, the largest groups were the posterior fossa groups, Pf_Epn_a ($N = 72$) and Pf_Epn_b ($N = 39$) followed by the supratentorial group (St_Epn_Rel) ($N = 49$). Among all 99 DUBs, *USP30* and *STAMBPL1* were most significantly different in these 3 EPN subgroups. *USP30* expression most significantly distinguished Pf_Epn_a and Pf_Epn_b, whereas *STAMBPL1* expression was decreased compared to the other subgroups (Figure 7).

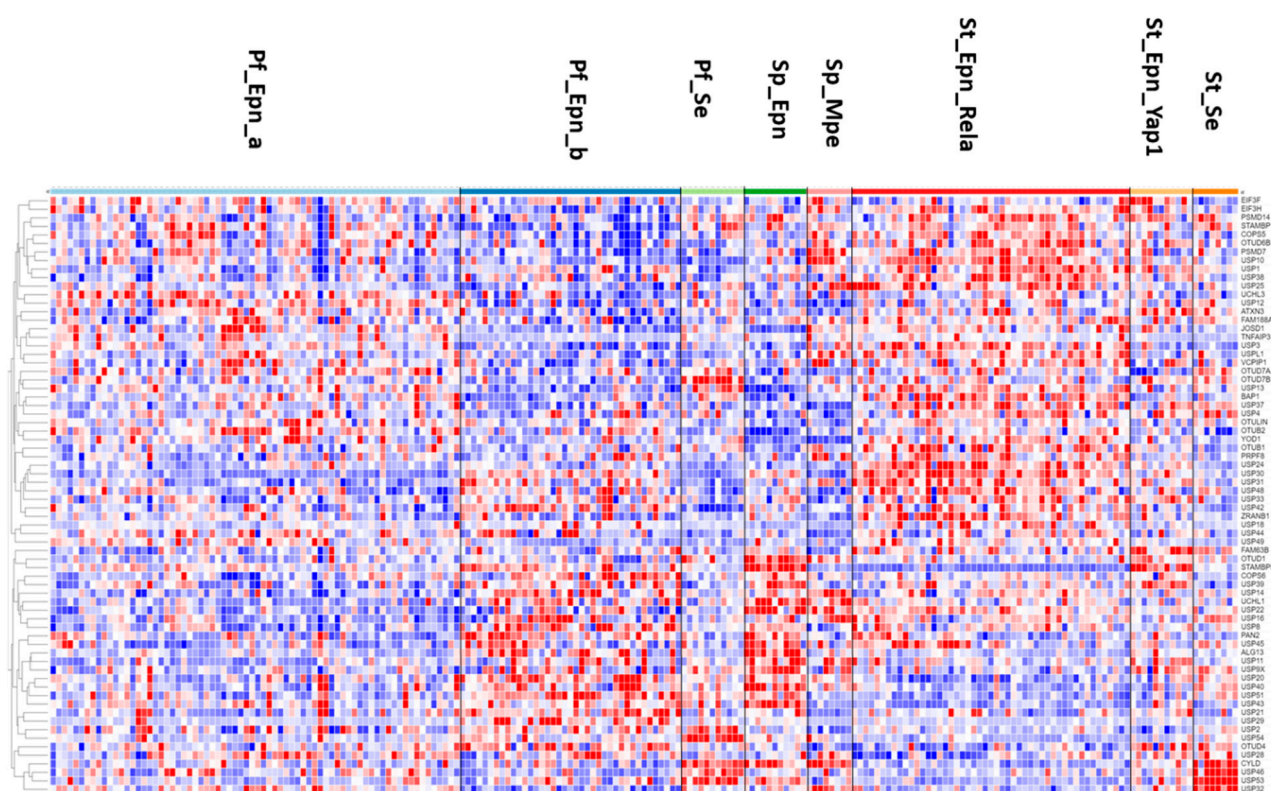


Figure 6. Heatmap and cluster analysis of DUB gene expression in ependymoma subtypes (Pf_Epn_a, N = 72; Pf_Epn-b, N = 39; Pf_se, N = 11; Sp_Epn, N = 11; Sp_Mpe, N = 8; St_Epn_Rel, N = 49; St_Epn_Yap1, N = 11; St_Se, N = 8).

The UPS30 protein is located on the mitochondrial outer membrane [85] and serves as an inhibitor of mitophagy [86,87] by blocking the action of the E3 ligase PARKIN [88]. STAMBPL1 is a K63-specific DUB reported to have higher expression in cancer tissue than in adjacent control tissues [89,90].

The heatmap of DUB expression in EPN subgroups (Figure 6) showed a cluster with relatively elevated DUB expression in the St_Rel, subgroup (red squares in heatmap) and a cluster in which DUB expression was relatively decreased (blue squares in heatmap). Cytoscape analysis of GO biological pathways identified several DUBs associated with *histone deubiquitination* in both clusters. This included the upregulated expression of *BAP1*, *USP25*, *USP3*, and *USP49* (red squares), and downregulated expression of *USP16*, *USP21*, *USP22*, and *USP51* (blue squares) (Figure 6). Cytoscape Reactome pathway analysis of differentially expressed DUB genes in Figure 6 identified the expression of three DUB genes, *CYLD*, *USP2*, and *USP21*, to be associated with the TRAF2:RIP1 complex in tumor necrosis factor receptor (TNFR) signaling and apoptosis. The UPS2 protein has been labeled a “master regulator of apoptosis” since USP2 can remove ubiquitin chains from RIP1 and TRAF2, regulate TNF-TNFR1-mediated cell death, and upregulate the transcription of I κ B α [91]. Like USP2, USP21 was also reported to deubiquitinate RIP1 [92] and the selective USP21 inhibitor compound BAY-805 may have therapeutic potential in cancer [93]. Both CYLD and TNFAIP3 have been shown to also contribute to the regulation of NF- κ B [79,81]. Notably, the supratentorial molecular subgroup St_Se of EPN was unique in that it showed increased expression of a cluster of four DUB genes, *CYLD*, *USP46*, *USP53*, and *USP32* (Figure 6). This may be considered a new gene signature for this WHO grade I subependymoma (Se) subgroup [94]. Among the significant differentially expressed DUBs in the EPN dataset, five DUB genes were associated with the *Regulation of ERAD pathway*, including *ATXN3*, *USP3*, *USP14*, *USP25*, and *OTUD2/YOD1*. Since the Pfister ependymoma dataset

did not include non-tumor subjects or survival data, these comparisons were not possible for the DUB genes.

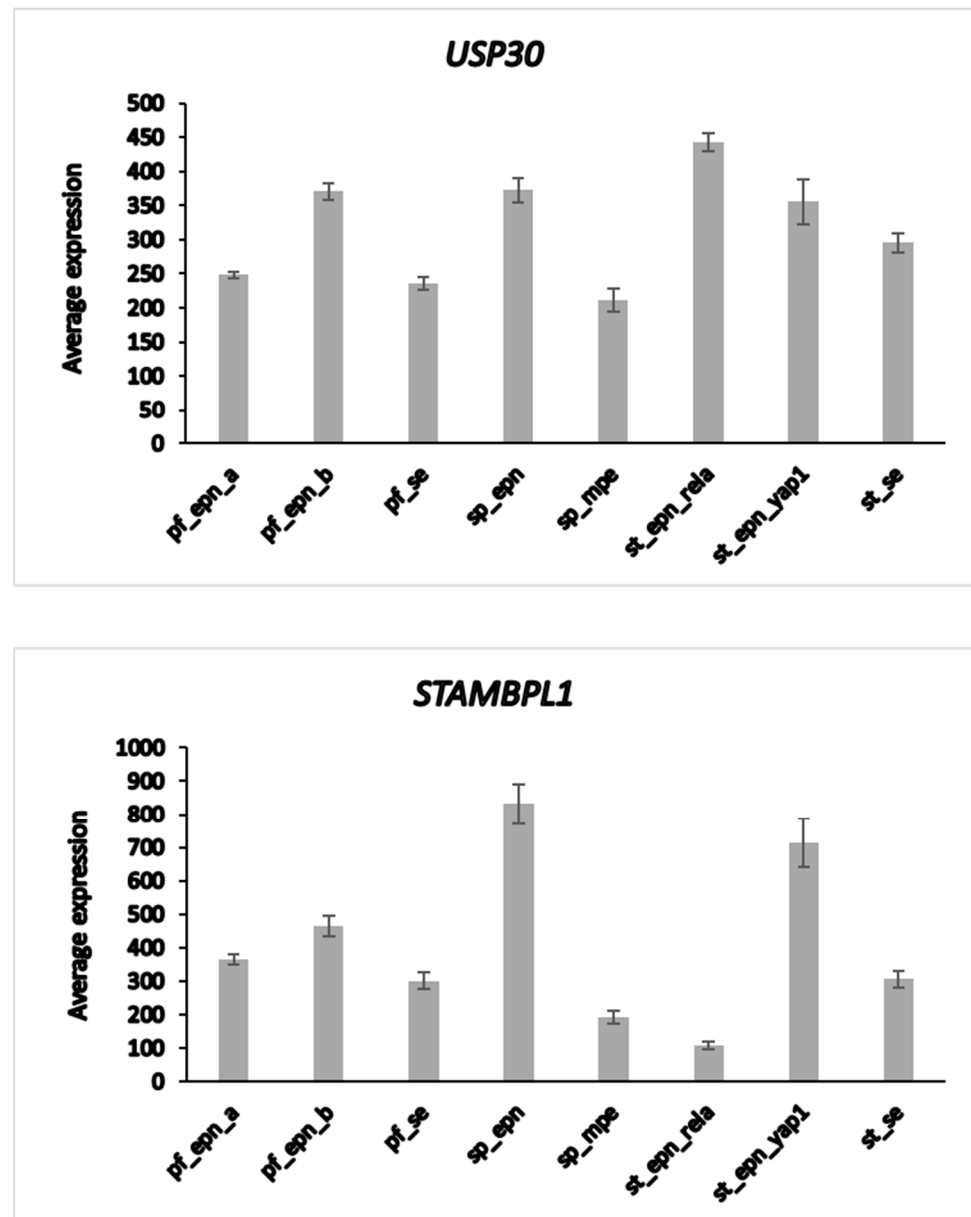


Figure 7. Differential expression of *USP30* and *STAMBPL1* in ependymoma molecular subgroups. *USP30*, $F = 12.58$, $p = 2.38 \times 10^{-13}$; *STAMBPL1*, $F = 54.29$, $p = 5.23 \times 10^{-43}$. This dataset is missing non-tumor control group for comparison by t-test.

3.9. DUBs in Craniopharyngioma

Of the 99 DUB genes analyzed, 39 DUBs were differentially expressed between normal brain and CPh. Other than DUB activity itself, *histone deubiquitination* (*USP3*, *USP7*, *USP16*) was the most significant GO pathway identified by Cytoscape.

USP13 ($F = 24.25$, $p = 1.00 \times 10^{-05}$) and *USP14* ($F = 11.88$, $p = 1.17 \times 10^{-03}$) expression were both decreased in CPh compared to non-tumor tissue (Figure 8). Of note, differential expression of *USP14* was also observed in mixed gliomas and in EPN. *USP14* protein was reported to be an inhibitor of the ERAD pathway by binding to IRE1a and inhibiting the phosphorylation of this ER stress-activated kinase [95].

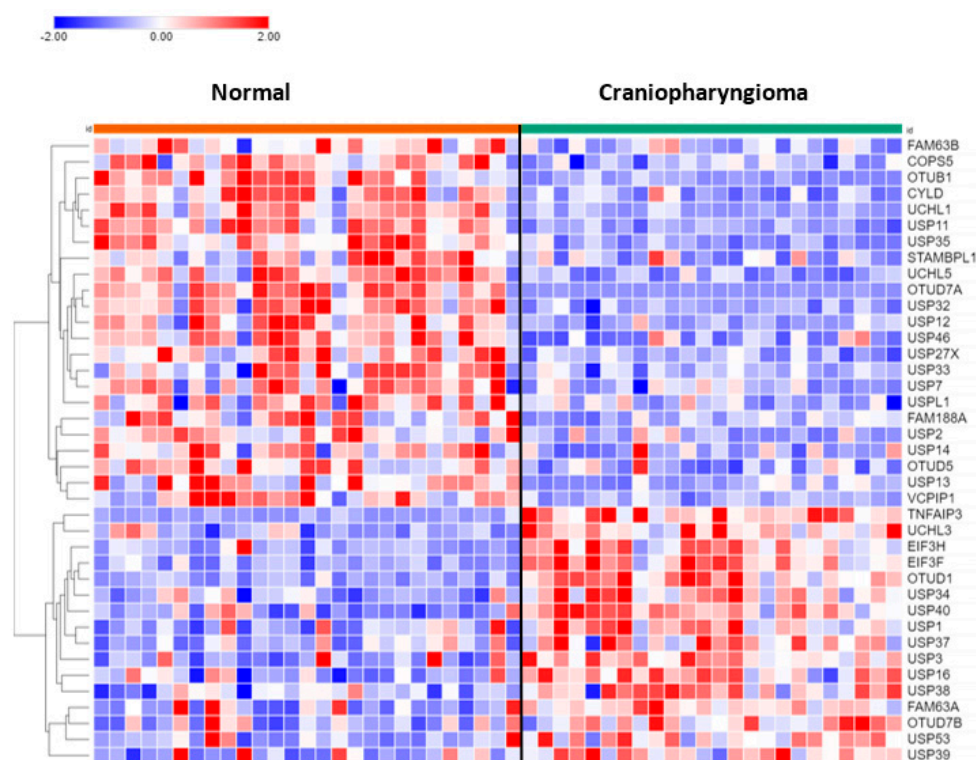


Figure 8. Heatmap and cluster analysis of DUB genes in craniopharyngioma. Normal, N = 27; Craniopharyngioma, N = 24.

3.10. DUB Regulation of Immune Response in Craniopharyngioma

In the dataset of CPh, the DUB genes *TNFAIP3*, *OTUD7A*, and *CYLD* were identified by Cytoscape to be associated with the *Regulation of immune response* pathway. *TNFAIP3* expression was upregulated about five-fold ($F = 78.84$, $p = 9.93 \times 10^{-12}$) compared to non-tumor tissue. *TNFAIP3* has been identified as a druggable target for melanoma in mice [96] and in inflammatory lung disease [97]. Expression of *OTUD7A* (aka Cezanne2) in CPh was significantly downregulated to 6.8% of normal non-tumor values ($F = 81.52$, $p = 5.34 \times 10^{-12}$). Located on chromosome 15, *OTUD7A* is one of six genes that contribute to the 15q13.3 microdeletion syndrome, which is associated with neurodevelopmental and psychiatric disorders [98,99]. Whether *OTUD7A* protein may qualify as a tumor suppressor for the development of CPh tumors (and gliomas, see above), as these data may suggest, requires further studies. Expression of the DUB and tumor suppressor *CYLD* was significantly reduced (>50%) in CPh compared to normal brain tissue. *CYLD* is an inhibitor of the immune response and NF- κ B signaling [100–102].

3.11. DUBs and Medulloblastoma

Seventy-eight of the ninety-nine DUB genes were differentially expressed ($p < 0.001$) among the four subgroups of MB. Table 4 shows the top ten DUB genes of each MB subgroup most significantly different from non-tumor tissues in the Swartling dataset. The heatmap in Figure 9 illustrates the distribution of DUB expression among the four MB subgroups (Group 3, Group 4, SHH, and WNT) in the Cavalli dataset. The most significant differentially expressed DUB gene by subgroups in the Cavalli dataset was *USP2* ($F = 271.00$, $p = 1.57 \times 10^{-119}$) (Figure 9), which was upregulated in Group 3 MB compared to the other subgroups. *USP2* protein removes ubiquitin from several proteins, including the E3 ubiquitin ligase *MDM2* [103], cyclin D (*CCND1*) [104], and the circadian clock protein *PER1* [105]. While the Cavalli MB dataset does not include non-tumor controls, the Donson dataset showed that *USP2* expression was elevated compared to the non-tumor brain. This was confirmed in the large meta-analysis of Weishaupt et al. [63] available in

the R2 genomics site as the Swartling dataset, which identified *USP2* as the most significant differentially expressed gene in the five groups (non-tumor, Group 3, Group 4, SHH, Wnt). The role of *USP2* in the deubiquitination of clock proteins regulating the circadian rhythm of pathways is well documented [106,107]. *USP2* may function as an oncogene in breast and gastric cancer by inhibiting autophagy and this DUB has been proposed as a therapeutic target in breast cancer [108,109]. *USP2* expression was also differentially expressed according to age groups ($F = 13.73$, $p = 1.01 \times 10^{-08}$). The age distribution for the four MB subgroups showed elevated *USP2* expression primarily in infants and children (Figure 10) and high expression of *USP2* was associated with poor survival (Table 4). *USP2* may be a lucrative therapeutic target in patients with Group 3 MB.

Table 4. Top ten differentially expressed DUB genes by MB subgroup compared to non-tumor group in the Swartling dataset.

Group 3 (N = 233)	DUB	p Value vs. Non-Tumor	Chromosome	Versus Non-Tumor Group in the Swartling Dataset
<i>USP46</i>	Usp	1.16×10^{-57}	4	Down
<i>USP2</i>	Usp	5.71×10^{-53}	11	Up
<i>PSMD14</i>	Jamm	4.25×10^{-51}	2	Up
<i>USP49</i>	Usp	1.34×10^{-36}	6	Up
<i>USP28</i>	Usp	2.41×10^{-26}	11	Down
<i>USP30</i>	Usp	1.29×10^{-25}	12	Up
<i>UCHL1</i>	Uch	1.72×10^{-22}	4	Down
<i>OTUD7A</i>	Otu	6.20×10^{-22}	15	Down
<i>USP44</i>	Usp	6.39×10^{-22}	12	Down
<i>COPS6</i>	Jamm	2.19×10^{-19}	7	Up
Group 4 (N = 530)				
<i>USP20</i>	Usp	8.96×10^{-65}	9	Up
<i>USP28</i>	Usp	2.28×10^{-63}	11	Down
<i>USP22</i>	Usp	1.35×10^{-61}	17	Up
<i>USP32</i>	Usp	1.21×10^{-58}	17	Up
<i>USP3</i>	Usp	2.98×10^{-54}	15	Down
<i>USP30</i>	Usp	2.19×10^{-52}	12	Up
<i>USP49</i>	Usp	1.49×10^{-43}	6	Up
<i>USP45</i>	Usp	9.56×10^{-36}	6	Down
<i>USP36</i>	Usp	7.95×10^{-29}	17	Up
<i>EIF3H</i>	Jamm	1.59×10^{-27}	8	Down
SHH (N = 405)				
<i>EIF3H</i>	Jamm	4.51×10^{-135}	8	Up
<i>USP2</i>	Usp	1.17×10^{-88}	11	Down
<i>USP20</i>	Usp	2.26×10^{-69}	9	Down
<i>CYLD</i>	Usp	7.13×10^{-64}	16	Down

Table 4. Cont.

Group 3 (N = 233)	DUB	p Value vs. Non-Tumor	Chromosome	Versus Non-Tumor Group in the Swartling Dataset
<i>USP25</i>	Usp	4.63×10^{-40}	21	Down
<i>USP32</i>	Usp	4.97×10^{-38}	17	Down
<i>USP33</i>	Usp	5.42×10^{-36}	1	Down
<i>JOSD1</i>	Mjd	2.40×10^{-30}	22	Up
<i>USP11</i>	Usp	3.32×10^{-28}	X	Down
<i>USP13</i>	Usp	1.03×10^{-26}	3	Up
WNT (N = 118)				
<i>UCHL1</i>	Uch	2.14×10^{-82}	4	Down
<i>USP2</i>	Usp	3.18×10^{-56}	11	Down
<i>USP20</i>	Usp	6.88×10^{-50}	9	Down
<i>USP32</i>	Usp	2.23×10^{-47}	17	Down
<i>USP5</i>	Usp	1.19×10^{-38}	12	Up
<i>COPS6</i>	Jamm	2.59×10^{-32}	7	Up
<i>EIF3H</i>	Jamm	1.19×10^{-29}	8	Up
<i>OTUD7A</i>	Otu	1.48×10^{-29}	15	Down
<i>USP33</i>	Usp	1.38×10^{-28}	1	Down
<i>USP28</i>	Usp	6.05×10^{-27}	11	Down

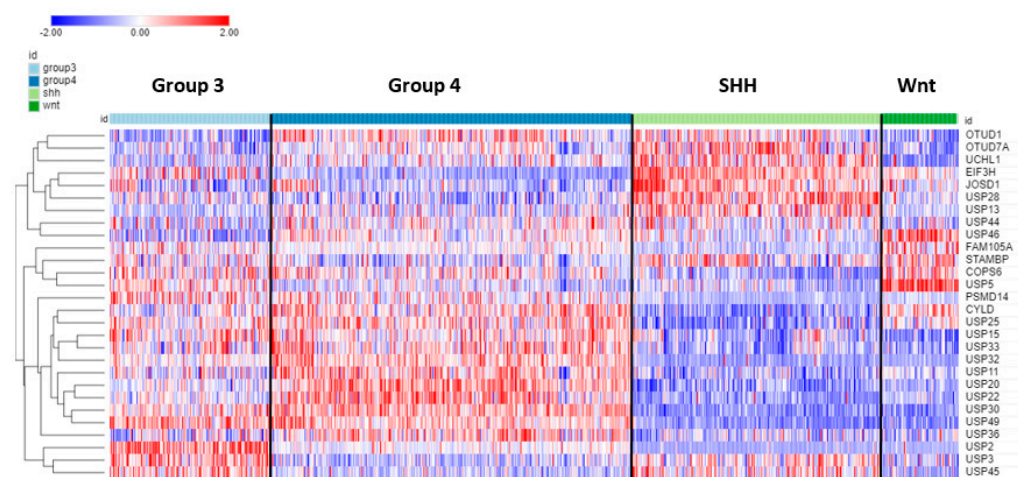


Figure 9. Heatmap and cluster analysis of the top 12 differentially expressed DUB genes for each of the 4 MB subgroups compared to non-tumor brain (note that due to overlap the total is less than 48). The Swartling dataset was used to identify top genes differing from non-tumor controls. The Cavalli dataset was used for the construction of the heatmap depicting the expression of these genes. Based on gene expression in the MB subgroups, the most significantly elevated DUBs for each group were Group 3—*USP2*; Group 4—*USP20*; SHH—*EIF3H*; WNT—*USP5*. Group 3, N = 144; Group 4, N = 326; SHH, N = 223; Wnt, N = 70).

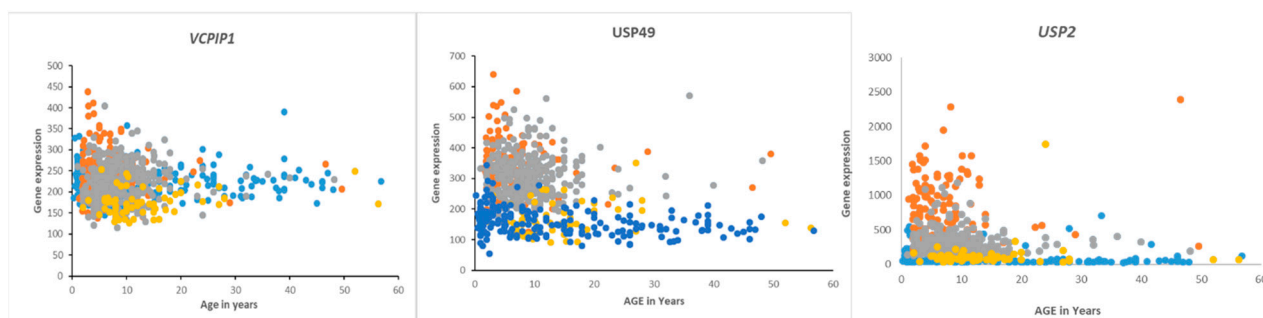


Figure 10. Gene expression of *VCPIP1*, *USP49*, and *USP2* in medulloblastoma by age and subgroups. Orange—Group 3, Gray—Group 4, Blue—SHH, Yellow—Wnt. Of these genes, *USP2* expression was most specifically elevated in Group 3 MB infants and children compared to the other groups (Cavalli dataset) and compared to a non-tumor group (Swartling dataset).

3.12. Survival in Medulloblastoma Subgroups and DUB Expression

Overall survival in the Cavalli dataset, as determined by the R2 genomics platform, was best in the Wnt group, worst in Group 3, and intermediate in SHH and Group 4, confirming previously determined survival times [62]. DUB genes that were significantly associated with survival ($p < 0.01$, for Kaplan Meier curves) are listed in Table 5 and includes DUB genes not differentially expressed between subgroups. DUB genes with the most significant Kaplan Meier curves (high vs low) and hazard ratios included *VCPIP1*, *USP49*, and *USP2*. High expression of these genes was associated with worse survival (Table 4). While high expression of *VCPIP1* was associated with worse survival in the Cavalli dataset, expression of *VCPIP1* in none of the four MB groups was significantly higher than in non-tumor tissues in the Swartling dataset. High expression of *USP49* was observed in infants and young children in Groups 3 and 4, whereas high expression of *USP2* was primarily observed in infants and young children in Group 3 (Figure 10).

Table 5. DUB gene expression and medulloblastoma survival data (Cavalli dataset).

DUB	DUB Family	Chromosome	Chi Square Kaplan Meier	p Value	Hazard Ratio	p Value for Hazard Ratio	Better Survival
<i>VCPIP1</i>	Otu	8	28.14	1.13×10^{-07}	1.9	1.10×10^{-05}	Low
<i>USP49</i>	Usp	6	26.73	2.34×10^{-07}	1.9	1.30×10^{-05}	Low
<i>USP2</i>	Usp	11	21.82	2.99×10^{-06}	1.3	3.50×10^{-05}	Low
<i>USP51</i>	Usp	X	19.36	1.08×10^{-05}	0.44	1.00×10^{-04}	High
<i>STAMBPL1</i>	Jamm	10	16.70	4.37×10^{-05}	0.73	3.10×10^{-04}	High
<i>PSMD14</i>	Jamm	2	18.05	2.16×10^{-05}	1.4	4.20×10^{-04}	Low
<i>ZRANB1</i>	Otu	10	17.11	3.52×10^{-05}	0.54	1.00×10^{-03}	High
<i>OTUD3</i>	Otu	1	18.76	1.48×10^{-05}	2.4	1.30×10^{-03}	Low
<i>PRPF8</i>	Jamm	17	18.77	1.47×10^{-05}	0.58	2.20×10^{-03}	High
<i>USP15</i>	Usp	12	16.42	5.06×10^{-05}	2	3.00×10^{-03}	Low
<i>USP45</i>	Usp	6	14.82	1.18×10^{-04}	1.5	3.90×10^{-03}	Low
<i>USP26</i>	Usp	X	22.77	1.82×10^{-06}	7.3	5.20×10^{-03}	Low
<i>USP36</i>	Usp	17	22.07	2.63×10^{-06}	2.2	5.50×10^{-03}	Low
<i>USPL1</i>	Usp	13	14.89	1.14×10^{-04}	2.1	5.80×10^{-03}	Low
<i>USP25</i>	Usp	21	12.36	4.39×10^{-04}	1.6	8.70×10^{-03}	Low
<i>EIF3H</i>	Jamm	8	13.23	2.75×10^{-04}	1.5	9.40×10^{-03}	Low
<i>COPS5</i>	Jamm	8	9.25	2.36×10^{-04}	1.9	9.90×10^{-03}	Low

3.13. Medulloblastoma DUBs and ERAD

Differential expression of several DUB genes (*USP13*, *USP14*, *USP25*, *USP19*, *OTUD2* (alias *YOD1*)) in the Cavalli dataset was associated with the GO category of *Regulation of ERAD pathway*. This list of genes includes three DUBs (*USP14*, *USP19*, *USP25*) shared with the list of differentially expressed ERAD genes in glioma (Table 3). *USP25* was the only ERAD-associated DUB gene among the top ten DUB genes in the SHH MB group (Table 4). Our data implicate both *USP25* and *USP13* with ERAD in the SHH group of MB (Figure 11). In the Swartling dataset, the expression of *USP25* was downregulated in the SHH group compared to non-tumor controls ($t = 14.37$, $p = 3.17 \times 10^{-41}$), while the expression of *USP13* was elevated compared to non-tumor tissues ($t = 11.36$, $p = 1.41 \times 10^{-27}$). Expression of *USP14*, but not *USP19* and *OTUD2*, was also reduced in the SHH group versus non-tumor tissues, but at a much lower level of significance ($t = 3.35$, $p = 8.64 \times 10^{-04}$).

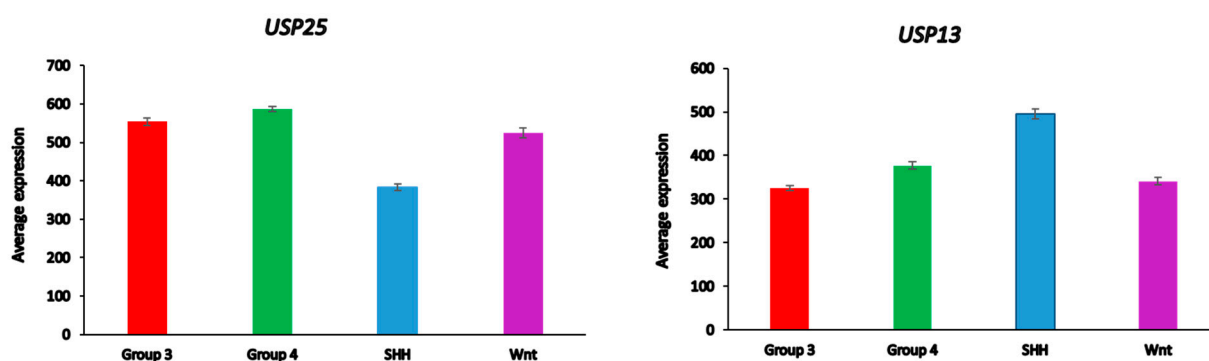


Figure 11. Differential expression of ERAD-associated DUBs in different medulloblastoma subgroups (Cavalli dataset). *USP25*, $F = 138.98$, $p = 9.08 \times 10^{-72}$; *USP13*, $F = 49.90$, $p = 1.93 \times 10^{-29}$.

3.14. Medulloblastoma DUBs and the Immune Response

Five differentially expressed DUB genes were associated with the GO category of *Regulation of immune response* in the Cavalli dataset. This included DUB genes *CYLD* ($F = 141.44$, $p = 8.53 \times 10^{-73}$), *PSMD14* ($F = 58.20$, $p = 7.15 \times 10^{-34}$), *OTUD7A* ($F = 66.35$, $p = 4.14 \times 10^{-38}$), *USP18* ($F = 37.27$, $p = 1.78 \times 10^{-22}$), and *PSMD7* ($F = 16.56$, $p = 1.96 \times 10^{-10}$). Table 6 shows the genes that were significantly elevated or decreased compared to non-tumor samples in the Swartling dataset.

CYLD is an inhibitor of the immune response, alters NF- κ B signaling, and affects the development and Th2 conversion of Treg cells [101,102,110]. *PSMD14* and *PSMD7* are DUB components of the proteasome and *PSMD14* is a druggable target that specifically deubiquitinates at K63 and suppresses autophagy by affecting vesicular retrograde transport from the Golgi to the ER [111,112]. *OTUD7A* contributes to neuronal development [77,78] and *USP18* regulates the immune response by binding to the interferon receptor *IFNAR2* [82].

3.15. Medulloblastoma DUBs and DNA Damage Repair

Twelve of the ninety-nine DUB genes were identified as differentially expressed in MB compared to non-tumor tissue ($p < 0.0001$) for the GO category of *DNA repair* in the Swartling dataset, including *USP1*, *OTUB1*, *UCHL5*, *USP7*, and *PSMD14* (aka *POH1*) (Table 7). The DUB proteins *USP1*, *OTUB1*, *UCHL5*, *USP7*, and *PSMD14* were reported to contribute to double-strand break repair, *USP1* to Fanconi anemia pathway, *USP1* and *USP7* to translesion repair, *USP7* and *USP47* to base excision repair, and *USP7* and *USP45* to nucleotide excision repair [83]. In addition, the *USP28* protein was also found to contribute to the DNA damage response [113]. A highly significant reduction in *USP28* expression in Group 3, Group 4, and Wnt MB groups (Table 7) may point to an impaired DNA damage response in these MB groups. *PSMD14* was the most significantly upregulated DUB gene in Group 3 MB (Table 7) [114]. A subtype-specific analysis revealed that *PSMD14* over-

expression was limited to selected subtypes of Group 3 (Group 3 beta and gamma) and Group 4 (Group 4 alpha).

Table 6. DUBs and GO category of “Regulation of immune response” by MB group compared to non-tumor group of Swartling dataset (n = 291).

DUB	Family	p Value Corrected FDR	Versus Non-Tumor Group in Swartling Dataset
Group 3 (n = 233)			
<i>PSMD14</i>	Jamm	8.74×10^{-52}	Up
<i>OTUD7A</i>	Otu	1.70×10^{-22}	Down
<i>TNFAIP3</i>	Otu	6.26×10^{-10}	Up
<i>CYLD</i>	Usp	3.54×10^{-08}	Down
Group 4 (n = 530)			
<i>PSMD14</i>	Jamm	2.23×10^{-26}	Up
<i>OTUD7A</i>	Otu	1.16×10^{-13}	Down
<i>CYLD</i>	Usp	7.04×10^{-10}	Up
<i>TNFAIP3</i>	Otu	5.67×10^{-09}	Up
SHH (n = 405)			
<i>CYLD</i>	Usp	1.95×10^{-64}	Down
<i>PSMD14</i>	Jamm	4.95×10^{-09}	Down
<i>TNFAIP3</i>	Otu	2.95×10^{-08}	Up
<i>PSMD7</i>	Jamm	5.19×10^{-08}	Up
Wnt (n = 118)			
<i>OTUD7A</i>	Otu	8.10×10^{-30}	Down
<i>PSMD7</i>	Jamm	3.89×10^{-25}	Up
<i>TNFAIP3</i>	Otu	2.40×10^{-10}	Down
<i>CYLD</i>	Usp	4.19×10^{-04}	Up
<i>PSMD14</i>	Jamm	8.99×10^{-04}	Up

Table 7. DUBs and GO category of DNA repair in MB groups compared to non-tumor group.

DUB	Family	p Value vs. NT Group Swartling	Versus Non-Tumor Group in Swartling Dataset
Group 3 vs. NT			
<i>PSMD14</i>	Jamm	2.27×10^{-51}	Up
<i>USP28</i>	Usp	1.07×10^{-26}	Down
<i>COPS6</i>	Jamm	1.30×10^{-21}	Up
<i>USP47</i>	Usp	3.96×10^{-15}	Down
<i>UCHL5</i>	Uch	6.12×10^{-14}	Up
<i>COPS5</i>	Jamm	1.61×10^{-10}	Up
<i>USP1</i>	Usp	2.53×10^{-06}	Up
<i>OTUB1</i>	Otu	3.33×10^{-05}	Down

Table 7. Cont.

DUB	Family	<i>p</i> Value vs. NT Group Swartling	Versus Non-Tumor Group in Swartling Dataset
Group 4 vs. NT			
<i>Usp28</i>	Usp	8.12×10^{-64}	Down
<i>USP3</i>	Usp	1.33×10^{-54}	Down
<i>USP45</i>	Usp	4.54×10^{-36}	Down
<i>PSMD14</i>	Jamm	1.45×10^{-26}	Up
<i>COPS6</i>	Jamm	3.10×10^{-24}	Up
<i>USP1</i>	Usp	1.48×10^{-16}	Up
<i>OTUB1</i>	Otu	1.67×10^{-14}	Down
<i>USP7</i>	Usp	2.65×10^{-12}	Up
<i>COPS5</i>	Jamm	4.01×10^{-06}	Down
<i>USP47</i>	Usp	2.16×10^{-04}	Down
<i>UCHL5</i>	Uch	2.11×10^{-03}	Up
SHH vs. NT			
<i>USP10</i>	Usp	2.21×10^{-15}	Up
<i>PSMD14</i>	Jamm	8.58×10^{-09}	Down
<i>COPS5</i>	Jamm	1.16×10^{-08}	Up
<i>USP45</i>	Usp	3.60×10^{-07}	Down
<i>UCHL5</i>	Uch	1.30×10^{-06}	Down
<i>USP3</i>	Usp	5.90×10^{-06}	Down
<i>COPS6</i>	Jamm	5.98×10^{-06}	Down
<i>USP1</i>	Usp	6.06×10^{-06}	Up
<i>USP47</i>	Usp	6.68×10^{-04}	Down
<i>USP7</i>	Usp	1.71×10^{-03}	Up
WNT vs. NT			
<i>COPS6</i>	Jamm	2.67×10^{-32}	Up
<i>USP28</i>	Usp	5.39×10^{-27}	Down
<i>USP3</i>	Usp	3.53×10^{-25}	Down
<i>USP45</i>	Usp	2.61×10^{-22}	Down
<i>UCHL5</i>	Usp	4.72×10^{-14}	Down
<i>USP10</i>	Usp	7.73×10^{-11}	Up
<i>COPS5</i>	Jamm	1.02×10^{-03}	Up
<i>PSMD14</i>	Jamm	1.46×10^{-03}	Up
<i>OTUB1</i>	Otu	2.89×10^{-03}	Up
<i>USP1</i>	Usp	4.55×10^{-03}	Up

3.16. DUBs in Neuroblastoma (Fischer Dataset)

The dataset of Fischer on NBT allowed the examination of DUB genes in patients with various treatments. Intensive chemotherapy of NBT was associated with increased expression of selected DUB genes and a decrease in several other DUB members compared to the observation group. Intriguingly, limited chemotherapy or surgery had no significant effect on the expression of DUB genes compared to the observation group alone (Figure 12).

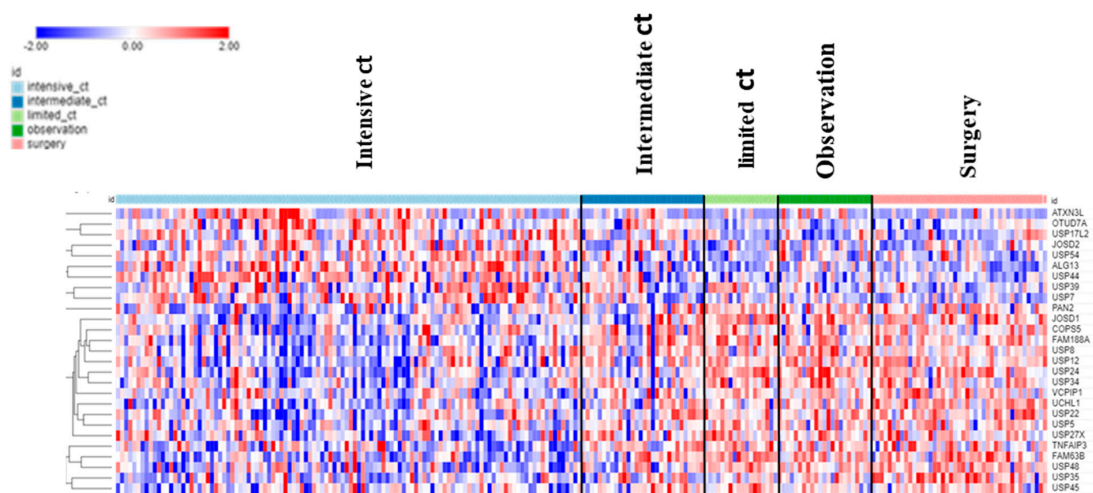


Figure 12. Treatment effects on DUB gene expression in Neuroblastoma. Intensive chemotherapy (ct) (N = 114), intermediate ct (N = 30), limited ct (N = 18), observation (no treatment control) (N = 23), surgery (N = 43).

Patients receiving intensive chemotherapy of their NBT showed significantly reduced tumor tissue expression of *USP24*, *USP34*, *MINDY2*, *USP8*, *JOSD1*, *USP52*, and *USP12* when compared to the observation group. The most significant differences in DUB expression between limited and intensive chemotherapy included *USP24*, *JOSD1*, and *MINDY2* (Figure 13). Notably, there were many other genes in the Fischer dataset that showed differential expression between the limited and intensive chemotherapy groups, the most significant of them being *MDGA1* ($F = 128.15$, $p = 4.24 \times 10^{-21}$) with approximately a four-fold difference. *MDGA1* is expressed mainly in neurons and astrocytes of the brain.

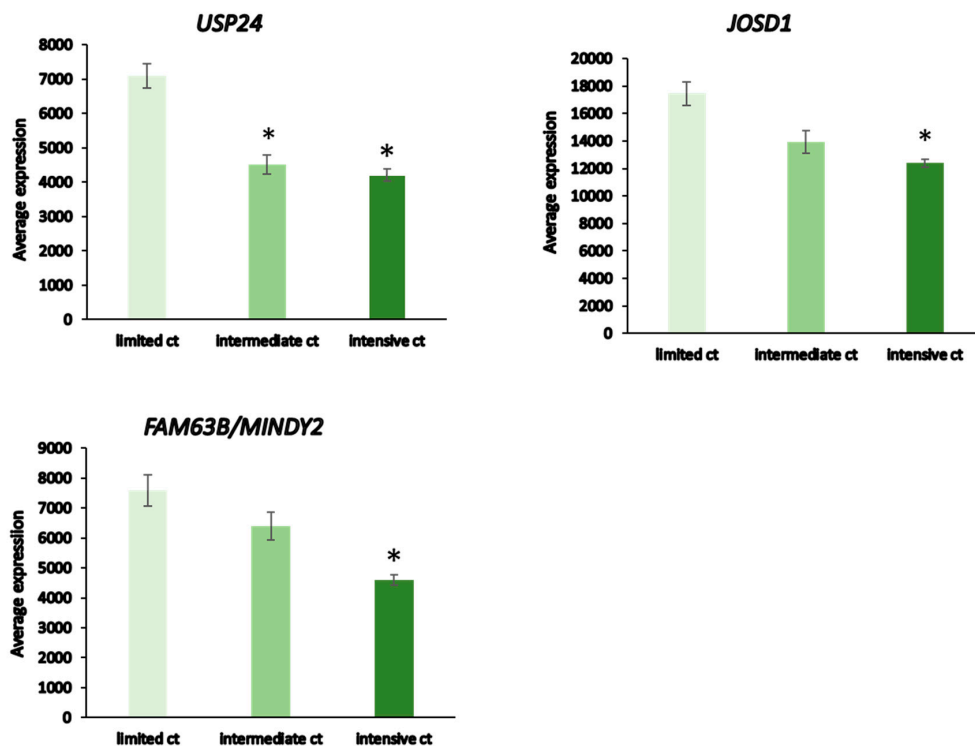


Figure 13. DUB expression in limited vs intensive chemotherapy of neuroblastoma from the Fischer dataset. Limited chemotherapy (ct), N = 18, intermediate ct, N = 30, intensive ct, N = 114. *USP24*, $F = 21.10$, $p = 7.44 \times 10^{-09}$; *JOSD1*, $F = 18.44$, $p = 6.26 \times 10^{-08}$; *MINDY2*, $F = 21.61$, $p = 4.99 \times 10^{-09}$. * significantly different from limited ct group at $p < 0.001$ by *t*-test.

4. Discussion

The complex functional roles of DUBs in tumor biology are gradually emerging [115]. Here, we present the first comprehensive gene expression profiling of 99 DUB family members in 6 different brain tumor entities that span different molecular subtypes and age groups. We also included gene expression data from different treatment groups of NBT, the most common extracranial sympathetic nervous system tumor in children, to better understand the emerging role of DUBs in pediatric and adult CNS tumors and the effect of treatment on DUB expression. While we observed pronounced gene expression changes for several DUBs, for brevity, we will only discuss those selected DUB members with the highest differential expression. Wherever possible, we have focused on known brain-related functions for these DUBs, with a particular emphasis on clinically relevant pathomechanisms, such as the ERAD pathway, immune system, and DNA damage repair.

GBM displayed a distinct downregulation of *USP46* and *ZRANB1*. Ubiquitously expressed throughout the mammalian brain, *USP46* is involved in the formation of synapses and neuronal morphogenesis by regulating both excitatory and inhibitory synaptic transmission [116]. By deubiquitinating K63 ubiquitinated glutamnergic AMPARs (α -amino-3-hydroxy-5methyl-4-isoxazolepropionic acid) receptors *GluA1* and *GluA2*, which are considered to mediate most of the excitatory synaptic transmission in the brain, *USP46* upregulates the intracellular trafficking, cell surface density, and signal intensity of AMPARs [116,117]. These receptors are critical for perivascular brain invasion, promote plasticity and growth of GBM, and coincide with poor prognosis [118–120]. *USP46* also interferes with the neuronal activity-dependent ubiquitination and trafficking of *GABA_A* receptors. Loss of *USP46* coincides with reduced expression of glutamic acid decarboxylase (*GAD67*) which synthesizes *GABA* [121]. Recently, higher expression of the non-coding (nc)RNA *USP46-AS1* has been linked to increased overall survival in glioma [122]. It is tempting to speculate that the marked reduction in *USP46* gene expression in GBM, but not AS, coincides with the acquisition of altered receptor density in the plasma membrane and synaptic activity during dedifferentiation from high-grade AS to GBM. *GABA_A* receptor activity was reported to inhibit glioma growth and the lowest levels of *GABA_A* receptors were reported in GBM compared to lower-grade glioma [123,124].

While the role of *ZRANB1* (zinc finger RANBP2-type containing 1, *TRABID*) in glioma is still unclear, it is likely multifactorial in nature. In breast cancer, this K29- and K33-specific DUB binds, deubiquitinates, and stabilizes the enhancer of zeste homologue (*EZH2*) catalytic component of the gene silencing Polycomb repressive complex 2 (*PRC2*) to promote growth, resulting in poor prognosis [66]. *USP1* in glioma [125], as well as *USP7* and *USP34*, also converge on *EZH2* to promote tumorigenesis [126]. Tight regulation of *ZRANB1* expression is critical in glioma. Reduced expression of *ZRANB1* may confer a survival advantage to GBM by reducing UPR through the recruitment of p62 to K33-ubiquitinated protein aggregates for autophagic removal [127]. However, in solid tumors, lower *ZRANB1* levels coincide with epigenetic regulation that promotes interferon and inflammatory immune cell responses in the tumor microenvironment [128–130]. Lower *ZRANB1* levels also attenuate the deubiquitination of K29-linked polyubiquitinated *53BP1*. Proteasomal removal of this DNA repair factor mitigates genomic instability by preventing *53BP1* from blocking homologous recombination repair at double-strand DNA breaks [131]. Further studies are needed to establish the role of *ZRANB1* in GBM.

Selected GBM, EPN, CPh, and MB subtypes showed distinct expression of specific DUB genes. Among 10 differentially expressed DUBs in the 3 GBM subtypes, only *TNFAIP3*, aka *A20*, was upregulated in mesenchymal GBM. Possessing both DUB and E3-ligase activities [132,133], *TNFAIP3* is an important player in a diverse array of diseases [134] and a key negative regulator of *NFkB* signaling downstream of *TNF* receptors, interleukin 1 receptor (*IL-1R*), pathogen recognition receptors (*PRRs*), *NOD*-like receptors (*NLRs*), *T*- and *B*-cell receptors, and *CD40* [135,136]. *TNFAIP3* regulates glioma stem cell survival, increases resistance to alkylating agents, and is considered a poor prognostic marker in GBM [137,138]. While *TNFAIP3* upregulation was a unique mesenchymal feature among GBM subtypes,

DUB genes significantly associated with immune cell functions were identified in other GBM subtypes, the St_se subgroup of EPN, MB, and in CPh. This included *TNFAIP3*, *CYLD* (*Cylindromatosis*), another negative regulator of NF- κ B signaling [102], and the critical neurodevelopmental factor and putative tumor suppressor *OTUD7A/Cezanne-2* [78]. These data suggest a redundant role for several DUBs in targeting NF- κ B signaling as a mechanism to regulate inflammatory and immune responses in intra- and extracranial nervous system brain tumors.

Among the four MB subgroups, we identified *USP2* to be selectively upregulated primarily in infants and children within Group 3 MB (Figure 9). Group 3 MB frequently have elevated MYC levels due to MYC overexpression or MYC gene amplifications and these patients have the worst prognosis of all MB groups with less than 50% survival [139,140]. In the Cavalli dataset, MYC expression was elevated most in the Group 3 gamma subtype. As may be expected, *USP2* DUB functions target a wide range of interconnected pathways in a tissue-specific manner [141]. Relevant *USP2* functions in tumorigenesis target the metabolic (e.g., fatty acids) and p53 pathways, EMT, cell cycle control, and maintenance of genome stability [141]. High *USP2* levels resulted in the downregulation of several miRs, including MYC-targeting miR-34b/c, which resulted in the deubiquitination of MDM2 and elevated MYC levels with subsequent p53 inactivation in prostate cancer cells [142]. Hence, it is conceivable that higher *USP2* expression may contribute to higher MYC protein levels in Group 3 MB patients.

Emerging research is starting to unravel the complex and clinically relevant relationships between UPR, ER, and DNA stress signaling, chronic inflammation, and immune responses in primary brain tumors and their microenvironment [143–146]. We identified a selected group of DUBs (*USP13*, *USP14*, *USP19*, *USP25*, *OTUD2/YOD1*) associated with the *Regulation of ERAD pathway* across several adult and pediatric primary brain tumors (GBM, EPN, CPh, MB). A recent TCGA-based gene expression profiling interactive analysis (GEPiA; <http://gepia.cancer-pku.cn/> (accessed on 25 August 2023)) of low-grade glioma and GBM identified lower expression of all but one (*USP25*) of these USP DUB members in GBM [147]. There was a strong correlation between higher expression of *USP14* and worse prognosis in GBM patients [147]. In addition to its roles in the ER [73], *USP14* (and *UCH37*) engages in polyubiquitin chain trimming which can delay proteasomal degradation by weakening the affinity of ubiquitin chains with ubiquitin-binding receptors at the proteasome [148]. Hence, *USP14* has been targeted with a small molecule inhibitor [149] or selected *USP14* aptamers [150] to enhance proteasomal activity and degradation of proteotoxicity. Although *USP14* downregulation in several tumor types was shown to reduce tumor burden in mice, data are lacking for brain tumors [151,152]. *OTUD2/YOD1* is another DUB with regulator functions in the ERAD pathway and is linked to injury-induced ER stress responses [153,154]. This includes a regulatory role of the inflammatory cytokine IL1 and p62 NF κ B signaling axis through interaction with the E3 ligase TRAF6 [155], which may contribute to *OTUD2/YOD1* deubiquitinating activity in attenuating neurogenic proteotoxicity [156]. In glioma, *OTUD2/YOD1* has been identified as a target of miR-190a-3p. Blocking miR-190a-3p or the overexpression of its target *OTUD2/YOD1* attenuated the proliferation and migration of glioma cells [157]. While the underlying mechanism is currently unknown, YAP and TAZ, the transcriptional coactivators and effectors of the Hippo signaling pathway, have been identified as downstream targets of an miR21-*OTUD2*-YAP/TAZ axis in hepatocellular carcinoma [158], thus, potentially linking *OTUD2/YOD1* to glioma stem cell maintenance and proliferation [159].

Among the selected DUBs significantly linked to the DNA damage repair pathway, the glioma and MB datasets shared several DUBs, including *USP1*, *USP47*, *UCHL5*, and *OTUD1*, which cover five major DNA damage repair pathways (BER, NER, FA, TLS, DSB) [83]. *USP1* targets *FANCD2/FANCI* to regulate the Fanconi anemia pathway (FA) [160] and, together with *USP7*, targets translesional DNA repair (TLS) [161,162]. *USP7*, a DDR-associated DUB exclusively altered in MB, and *USP47* target the base excision repair pathway (BER) [163,164], while *USP7* and *USP45* have regulatory roles in nucleotide ex-

cision repair (NER) [165,166]. *UCHL5* and *OTUD1* were reported to increase or decrease double-strand break repair (DSB), respectively [167,168]. Expressed among the top genes in Group 3 MB and highly significantly associated with poor survival in MB Groups 3 and 4 (Tables 4 and 5), *PSMD14* (aka *POH1*) was also significantly associated with immune responses and DNA repair, particularly in MB Groups 3 and 4 (Tables 6 and 7). *PSMD14* was shown to fortify tumor cells against DNA-damaging drugs by promoting a switch from error-prone non-homologous end-joining to homologous recombination [169,170]. This identifies proteasomal *PSMD14* as a key DUB in regulating ubiquitin conjugation in response to DNA damage and exemplifies the intricate relationships between the proteasome and DNA damage responses.

Changes in DUB expression also occurred during the treatment of extracranial NBT sympathetic nervous tumors. Our analysis of a dataset from NBT undergoing different treatment options identified significantly reduced expression of seven (*USP24*, *USP34*, *MINDY2*, *USP8*, *JOSD1*, *USP52*, *USP12*) DUBs in the treated versus non-treated NBT group. Intriguingly, *USP24*, *JOSD1*, and *MINDY2* showed the most significant downregulation during intensive versus limited chemotherapy (Figure 12). *USP24* has recently been identified as a novel tumor suppressor in NBT that targets collapsin response mediator protein 2 (CRMP2), which promotes axon growth, guidance, and neuronal polarity but also affects T cell polarization and migration [171,172]. Deubiquitination of CRMP2 by *USP24* ensured proper spindle pole assembly and blocked chromosomal instability and aneuploidy observed upon *USP24* knockdown in NBT [173]. A glimpse into possible additional cellular strategies in response to intensive treatment regimes in NBT cells comes from findings that *USP24* downregulation increases autophagy flux in cells [174]. The biological roles of Machado–Joseph DUB member *JOSD1* are complex [23]. While data on *JOSD1* in NBT are lacking, *JOSD1* can deubiquitinate and stabilize Snail protein to promote EMT and tissue invasion of lung cancer cells [175]. A small molecule inhibitor of *JOSD1* was shown to induce cell death of JAK2-V617F-positive primary acute myeloid leukemia (AML) cells [176]. Downregulation of *JOSD1* in treated NBT may also affect regulatory mechanisms of interferon-1 mediated inflammatory cytokine responses [177]. The role of the evolutionarily conserved *MINDY1/2* family of DUBs in brain tumors is currently unknown. However, *MINDY1* DUB activity promotes the proliferation of bladder cancer cells by stabilizing *MINDY1* interaction partner YAP protein and critical transcriptional regulator of the Hippo pathway. YAP overexpression in *MINDY1*-depleted cells was able to rescue this proliferation [178]. In human breast cancer cells, *MINDY1* stabilizes estrogen receptor alpha (ERα) and promotes Era-mediated proliferation [179].

5. Summary and Conclusions

In the current study, we have identified DUB coding genes and biological pathways that are statistically associated with CNS tumors. Several DUBs were specific for a particular CNS tumor or subgroup/subtype and others were common to two or more tumors. The *histone deubiquitination* GO pathway was over-represented in glioma, EPN, MB, CPh, and NBT datasets. The *DNA synthesis in DNA repair* and *regulation of ERAD pathways* were over-represented in DUB transcriptomes of MB and EPN, while various aspects of the immune response were associated with differential expression of DUBs in CNS tumors. For datasets that included survival data (mixed glioma and MB datasets), we identified DUB genes associated with significant hazard ratios. In conclusion, the role of DUBs as relevant modulators of cellular and immunoregulatory pathways in brain tumors is evolving. Selective DUB targeting strategies may provide important synergistic therapeutic potential in the future.

Author Contributions: Conceptualization, T.K. and J.V.; methodology, J.V.; formal analysis, J.V.; data curation, J.V.; writing—original draft preparation, T.K. and J.V.; writing—review and editing, T.K., S.H.-K., S.E.L. and J.V.; visualization, J.V. and T.K.; project administration, J.V. All authors have read and agreed to the published version of the manuscript.

Funding: TK is grateful to the Natural Sciences and Engineering Council of Canada (NSERC) for program grant funding (RGPIN-2023-04286).

Institutional Review Board Statement: Not applicable.

Informed Consent Statement: Not applicable.

Data Availability Statement: The data referred to in this manuscript are publicly available at the R2 Genomics Analysis and Visualization Platform (<http://r2.amc.nl> (accessed on 5 September 2023)) and at the NIH GEO database and are available upon reasonable request from the first author.

Conflicts of Interest: The authors declare no conflict of interest.

References

1. Gao, T.; Liu, Z.; Wang, Y.; Cheng, H.; Yang, Q.; Guo, A.; Ren, J.; Xue, Y. UUCD: A family-based database of ubiquitin and ubiquitin-like conjugation. *Nucleic Acids Res.* **2013**, *41*, D445–D451. [[CrossRef](#)]
2. van der Veen, A.G.; Ploegh, H.L. Ubiquitin-like proteins. *Annu. Rev. Biochem.* **2012**, *81*, 323–357. [[CrossRef](#)]
3. Varshavsky, A. The Ubiquitin System, Autophagy, and Regulated Protein Degradation. *Annu. Rev. Biochem.* **2017**, *86*, 123–128. [[CrossRef](#)] [[PubMed](#)]
4. Dikic, I.; Schulman, B.A. An expanded lexicon for the ubiquitin code. *Nat. Rev. Mol. Cell Biol.* **2023**, *24*, 273–287. [[CrossRef](#)] [[PubMed](#)]
5. Swatek, K.N.; Komander, D. Ubiquitin modifications. *Cell Res.* **2016**, *26*, 399–422. [[CrossRef](#)] [[PubMed](#)]
6. Tracz, M.; Bialek, W. Beyond K48 and K63: Non-canonical protein ubiquitination. *Cell. Mol. Biol. Lett.* **2021**, *26*, 1. [[CrossRef](#)]
7. Jacobson, A.D.; Zhang, N.Y.; Xu, P.; Han, K.J.; Noone, S.; Peng, J.; Liu, C.W. The lysine 48 and lysine 63 ubiquitin conjugates are processed differently by the 26 s proteasome. *J. Biol. Chem.* **2009**, *284*, 35485–35494. [[CrossRef](#)]
8. Kwon, Y.T.; Ciechanover, A. The Ubiquitin Code in the Ubiquitin-Proteasome System and Autophagy. *Trends Biochem. Sci.* **2017**, *42*, 873–886. [[CrossRef](#)]
9. Dosa, A.; Csizmadia, T. The role of K63-linked polyubiquitin in several types of autophagy. *Biol. Futur.* **2022**, *73*, 137–148. [[CrossRef](#)]
10. Liu, Z.; Gong, Z.; Jiang, W.X.; Yang, J.; Zhu, W.K.; Guo, D.C.; Zhang, W.P.; Liu, M.L.; Tang, C. Lys63-linked ubiquitin chain adopts multiple conformational states for specific target recognition. *eLife* **2015**, *4*, e05767. [[CrossRef](#)]
11. Suresh, H.G.; Pascoe, N.; Andrews, B. The structure and function of deubiquitinases: Lessons from budding yeast. *Open Biol.* **2020**, *10*, 200279. [[CrossRef](#)] [[PubMed](#)]
12. Mevissen, T.E.T.; Komander, D. Mechanisms of Deubiquitinase Specificity and Regulation. *Annu. Rev. Biochem.* **2017**, *86*, 159–192. [[CrossRef](#)] [[PubMed](#)]
13. Komander, D.; Clague, M.J.; Urbe, S. Breaking the chains: Structure and function of the deubiquitinases. *Nat. Rev. Mol. Cell Biol.* **2009**, *10*, 550–563. [[CrossRef](#)]
14. Lange, S.M.; Armstrong, L.A.; Kulathu, Y. Deubiquitinases: From mechanisms to their inhibition by small molecules. *Mol. Cell* **2022**, *82*, 15–29. [[CrossRef](#)] [[PubMed](#)]
15. Deng, L.; Meng, T.; Chen, L.; Wei, W.; Wang, P. The role of ubiquitination in tumorigenesis and targeted drug discovery. *Signal Transduct. Target. Ther.* **2020**, *5*, 11. [[CrossRef](#)] [[PubMed](#)]
16. Davis, M.I.; Simeonov, A. Ubiquitin-Specific Proteases as Druggable Targets. *Drug Target Rev.* **2015**, *2*, 60–64.
17. Rong, C.; Zhou, R.; Wan, S.; Su, D.; Wang, S.L.; Hess, J. Ubiquitin Carboxyl-Terminal Hydrolases and Human Malignancies: The Novel Prognostic and Therapeutic Implications for Head and Neck Cancer. *Front. Oncol.* **2020**, *10*, 592501. [[CrossRef](#)]
18. Johnston, S.C.; Riddle, S.M.; Cohen, R.E.; Hill, C.P. Structural basis for the specificity of ubiquitin C-terminal hydrolases. *EMBO J.* **1999**, *18*, 3877–3887. [[CrossRef](#)]
19. Larsen, C.N.; Price, J.S.; Wilkinson, K.D. Substrate binding and catalysis by ubiquitin C-terminal hydrolases: Identification of two active site residues. *Biochemistry* **1996**, *35*, 6735–6744. [[CrossRef](#)]
20. Makarova, K.S.; Aravind, L.; Koonin, E.V. A novel superfamily of predicted cysteine proteases from eukaryotes, viruses and Chlamydia pneumoniae. *Trends Biochem. Sci.* **2000**, *25*, 50–52. [[CrossRef](#)]
21. Du, J.; Fu, L.; Sui, Y.; Zhang, L. The function and regulation of OTU deubiquitinases. *Front. Med.* **2020**, *14*, 542–563. [[CrossRef](#)]
22. Schluter, D.; Schulze-Niemand, E.; Stein, M.; Naumann, M. Ovarian tumor domain proteases in pathogen infection. *Trends Microbiol.* **2022**, *30*, 22–33. [[CrossRef](#)] [[PubMed](#)]
23. Zeng, C.; Zhao, C.; Ge, F.; Li, Y.; Cao, J.; Ying, M.; Lu, J.; He, Q.; Yang, B.; Dai, X.; et al. Machado-Joseph Deubiquitinases: From Cellular Functions to Potential Therapy Targets. *Front. Pharmacol.* **2020**, *11*, 1311. [[CrossRef](#)] [[PubMed](#)]
24. Patterson-Fortin, J.; Shao, G.; Bretscher, H.; Messick, T.E.; Greenberg, R.A. Differential regulation of JAMM domain deubiquitinating enzyme activity within the RAP80 complex. *J. Biol. Chem.* **2010**, *285*, 30971–30981. [[CrossRef](#)]
25. Pan, X.; Wu, S.; Wei, W.; Chen, Z.; Wu, Y.; Gong, K. Structural and Functional Basis of JAMM Deubiquitinating Enzymes in Disease. *Biomolecules* **2022**, *12*, 910. [[CrossRef](#)] [[PubMed](#)]
26. Dubiel, W.; Chaithongyot, S.; Dubiel, D.; Naumann, M. The COP9 Signalosome: A Multi-DUB Complex. *Biomolecules* **2020**, *10*, 1082. [[CrossRef](#)] [[PubMed](#)]

27. Abdul Rehman, S.A.; Kristariyanto, Y.A.; Choi, S.Y.; Nkosi, P.J.; Weidlich, S.; Labib, K.; Hofmann, K.; Kulathu, Y. MINDY-1 Is a Member of an Evolutionarily Conserved and Structurally Distinct New Family of Deubiquitinating Enzymes. *Mol. Cell* **2016**, *63*, 146–155. [[CrossRef](#)]
28. Hickey, C.M.; Wilson, N.R.; Hochstrasser, M. Function and regulation of SUMO proteases. *Nat. Rev. Mol. Cell Biol.* **2012**, *13*, 755–766. [[CrossRef](#)]
29. Tokarz, P.; Wozniak, K. SENP Proteases as Potential Targets for Cancer Therapy. *Cancers* **2021**, *13*, 2059. [[CrossRef](#)]
30. Mendoza, H.M.; Shen, L.N.; Botting, C.; Lewis, A.; Chen, J.; Ink, B.; Hay, R.T. NEDP1, a highly conserved cysteine protease that deNEDDylates Cullins. *J. Biol. Chem.* **2003**, *278*, 25637–25643. [[CrossRef](#)]
31. Qu, J.; Zou, T.; Lin, Z. The Roles of the Ubiquitin-Proteasome System in the Endoplasmic Reticulum Stress Pathway. *Int. J. Mol. Sci.* **2021**, *22*, 1526. [[CrossRef](#)]
32. Shibata, Y.; Voeltz, G.K.; Rapoport, T.A. Rough sheets and smooth tubules. *Cell* **2006**, *126*, 435–439. [[CrossRef](#)] [[PubMed](#)]
33. Schwarz, D.S.; Blower, M.D. The endoplasmic reticulum: Structure, function and response to cellular signaling. *Cell. Mol. Life Sci.* **2016**, *73*, 79–94. [[CrossRef](#)] [[PubMed](#)]
34. Almanza, A.; Carlesso, A.; Chinthala, C.; Creedican, S.; Doultzinos, D.; Leuzzi, B.; Luis, A.; McCarthy, N.; Montibeller, L.; More, S.; et al. Endoplasmic reticulum stress signalling—From basic mechanisms to clinical applications. *FEBS J.* **2019**, *286*, 241–278. [[CrossRef](#)] [[PubMed](#)]
35. He, B. Viruses, endoplasmic reticulum stress, and interferon responses. *Cell Death Differ.* **2006**, *13*, 393–403. [[CrossRef](#)]
36. Shen, J.; Chen, X.; Hendershot, L.; Prywes, R. ER stress regulation of ATF6 localization by dissociation of BiP/GRP78 binding and unmasking of Golgi localization signals. *Dev. Cell* **2002**, *3*, 99–111. [[CrossRef](#)]
37. Bertolotti, A.; Zhang, Y.; Hendershot, L.M.; Harding, H.P.; Ron, D. Dynamic interaction of BiP and ER stress transducers in the unfolded-protein response. *Nat. Cell Biol.* **2000**, *2*, 326–332. [[CrossRef](#)]
38. Madden, E.; Logue, S.E.; Healy, S.J.; Manie, S.; Samali, A. The role of the unfolded protein response in cancer progression: From oncogenesis to chemoresistance. *Biol. Cell* **2019**, *111*, 1–17. [[CrossRef](#)]
39. Park, J.; Cho, J.; Song, E.J. Ubiquitin-proteasome system (UPS) as a target for anticancer treatment. *Arch. Pharmacol Res.* **2020**, *43*, 1144–1161. [[CrossRef](#)]
40. Jurkovicova, D.; Neophytou, C.M.; Gasparovic, A.C.; Goncalves, A.C. DNA Damage Response in Cancer Therapy and Resistance: Challenges and Opportunities. *Int. J. Mol. Sci.* **2022**, *23*, 14672. [[CrossRef](#)] [[PubMed](#)]
41. Pilger, D.; Seymour, L.W.; Jackson, S.P. Interfaces between cellular responses to DNA damage and cancer immunotherapy. *Genes Dev.* **2021**, *35*, 602–618. [[CrossRef](#)]
42. Vriend, J.; Klönisch, T. Genes of the Ubiquitin Proteasome System Qualify as Differential Markers in Malignant Glioma of Astrocytic and Oligodendroglial Origin. *Cell. Mol. Neurobiol.* **2023**, *43*, 1425–1452. [[CrossRef](#)] [[PubMed](#)]
43. Vriend, J.; Thanasupawat, T.; Sinha, N.; Klönisch, T. Ubiquitin Proteasome Gene Signatures in Ependymoma Molecular Subtypes. *Int. J. Mol. Sci.* **2022**, *23*, 12330. [[CrossRef](#)] [[PubMed](#)]
44. Maris, J.M.; Hogarty, M.D.; Bagatell, R.; Cohn, S.L. Neuroblastoma. *Lancet* **2007**, *369*, 2106–2120. [[CrossRef](#)] [[PubMed](#)]
45. Park, J.R.; Bagatell, R.; London, W.B.; Maris, J.M.; Cohn, S.L.; Mattay, K.K.; Hogarty, M.; on behalf of the COG Neuroblastoma Committee. Children’s Oncology Group’s 2013 blueprint for research: Neuroblastoma. *Pediatr. Blood Cancer* **2013**, *60*, 985–993. [[CrossRef](#)] [[PubMed](#)]
46. Das, S.; Ramakrishna, S.; Kim, K.S. Critical Roles of Deubiquitinating Enzymes in the Nervous System and Neurodegenerative Disorders. *Mol. Cells* **2020**, *43*, 203–214. [[CrossRef](#)] [[PubMed](#)]
47. Maksoud, S. The Role of the Ubiquitin Proteasome System in Glioma: Analysis Emphasizing the Main Molecular Players and Therapeutic Strategies Identified in Glioblastoma Multiforme. *Mol. Neurobiol.* **2021**, *58*, 3252–3269. [[CrossRef](#)]
48. Sonoda, Y.; Ozawa, T.; Aldape, K.D.; Deen, D.F.; Berger, M.S.; Pieper, R.O. Akt pathway activation converts anaplastic astrocytoma to glioblastoma multiforme in a human astrocyte model of glioma. *Cancer Res.* **2001**, *61*, 6674–6678.
49. Molinaro, A.M.; Taylor, J.W.; Wiencke, J.K.; Wrensch, M.R. Genetic and molecular epidemiology of adult diffuse glioma. *Nat. Rev. Neurol.* **2019**, *15*, 405–417. [[CrossRef](#)] [[PubMed](#)]
50. Kim, H.J.; Park, J.W.; Lee, J.H. Genetic Architectures and Cell-of-Origin in Glioblastoma. *Front. Oncol.* **2020**, *10*, 615400. [[CrossRef](#)] [[PubMed](#)]
51. Ruda, R.; Bruno, F.; Pellerino, A.; Soffietti, R. Ependymoma: Evaluation and Management Updates. *Curr. Oncol. Rep.* **2022**, *24*, 985–993. [[CrossRef](#)] [[PubMed](#)]
52. Bou Zerdan, M.; Assi, H.I. Oligodendroglioma: A Review of Management and Pathways. *Front. Mol. Neurosci.* **2021**, *14*, 722396. [[CrossRef](#)]
53. Williamson, D.; Schwalbe, E.C.; Hicks, D.; Aldinger, K.A.; Lindsey, J.C.; Crosier, S.; Richardson, S.; Goddard, J.; Hill, R.M.; Castle, J.; et al. Medulloblastoma group 3 and 4 tumors comprise a clinically and biologically significant expression continuum reflecting human cerebellar development. *Cell Rep.* **2022**, *40*, 111162. [[CrossRef](#)] [[PubMed](#)]
54. Funakoshi, Y.; Sugihara, Y.; Uneda, A.; Nakashima, T.; Suzuki, H. Recent advances in the molecular understanding of medulloblastoma. *Cancer Sci.* **2023**, *114*, 741–749. [[CrossRef](#)] [[PubMed](#)]
55. Rechberger, J.S.; Toll, S.A.; Vanbilloen, W.J.F.; Daniels, D.J.; Khatua, S. Exploring the Molecular Complexity of Medulloblastoma: Implications for Diagnosis and Treatment. *Diagnostics* **2023**, *13*, 2398. [[CrossRef](#)]

56. Alomari, A.K.; Kelley, B.J.; Damisah, E.; Marks, A.; Hui, P.; DiLuna, M.; Vortmeyer, A. Craniopharyngioma arising in a Rathke's cleft cyst: Case report. *J. Neurosurg. Pediatr.* **2015**, *15*, 250–254. [[CrossRef](#)]
57. Johnsen, J.I.; Dyberg, C.; Wickstrom, M. Neuroblastoma—A Neural Crest Derived Embryonal Malignancy. *Front. Mol. Neurosci.* **2019**, *12*, 9. [[CrossRef](#)]
58. Qiu, B.; Matthay, K.K. Advancing therapy for neuroblastoma. *Nat. Rev. Clin. Oncol.* **2022**, *19*, 515–533. [[CrossRef](#)]
59. Mallepalli, S.; Gupta, M.K.; Vadde, R. Neuroblastoma: An Updated Review on Biology and Treatment. *Curr. Drug Metab.* **2019**, *20*, 1014–1022. [[CrossRef](#)]
60. Chung, C.; Boterberg, T.; Lucas, J.; Panoff, J.; Valteau-Couanet, D.; Hero, B.; Bagatell, R.; Hill-Kayser, C.E. Neuroblastoma. *Pediatr. Blood Cancer* **2021**, *68* (Suppl. S2), e28473. [[CrossRef](#)]
61. Gravendeel, L.A.; Kouwenhoven, M.C.; Gevaert, O.; de Rooij, J.J.; Stubbs, A.P.; Duijm, J.E.; Daemen, A.; Bleeker, F.E.; Bralten, L.B.; Kloosterhof, N.K.; et al. Intrinsic gene expression profiles of gliomas are a better predictor of survival than histology. *Cancer Res.* **2009**, *69*, 9065–9072. [[CrossRef](#)] [[PubMed](#)]
62. Cavalli, F.M.G.; Remke, M.; Rampasek, L.; Peacock, J.; Shih, D.J.H.; Luu, B.; Garzia, L.; Torchia, J.; Nor, C.; Morrissy, A.S.; et al. Intertumoral Heterogeneity within Medulloblastoma Subgroups. *Cancer Cell* **2017**, *31*, 737–754.e6. [[CrossRef](#)] [[PubMed](#)]
63. Weishaupt, H.; Johansson, P.; Sundstrom, A.; Lubovac-Pilav, Z.; Olsson, B.; Nelander, S.; Swartling, F.J. Batch-normalization of cerebellar and medulloblastoma gene expression datasets utilizing empirically defined negative control genes. *Bioinformatics* **2019**, *35*, 3357–3364. [[CrossRef](#)] [[PubMed](#)]
64. Ackermann, S.; Cartolano, M.; Hero, B.; Welte, A.; Kahlert, Y.; Roderwieser, A.; Bartenhagen, C.; Walter, E.; Gecht, J.; Kerschke, L.; et al. A mechanistic classification of clinical phenotypes in neuroblastoma. *Science* **2018**, *362*, 1165–1170. [[CrossRef](#)]
65. Seifert, M.; Schackert, G.; Temme, A.; Schrock, E.; Deutsch, A.; Klink, B. Molecular Characterization of Astrocytoma Progression Towards Secondary Glioblastomas Utilizing Patient-Matched Tumor Pairs. *Cancers* **2020**, *12*, 1696. [[CrossRef](#)]
66. Zhang, P.; Xiao, Z.; Wang, S.; Zhang, M.; Wei, Y.; Hang, Q.; Kim, J.; Yao, F.; Rodriguez-Aguayo, C.; Ton, B.N.; et al. ZRANB1 Is an EZH2 Deubiquitinase and a Potential Therapeutic Target in Breast Cancer. *Cell Rep.* **2018**, *23*, 823–837. [[CrossRef](#)]
67. Duan, R.; Du, W.; Guo, W. EZH2: A novel target for cancer treatment. *J. Hematol. Oncol.* **2020**, *13*, 104. [[CrossRef](#)]
68. Straining, R.; Eighmy, W. Tazemetostat: EZH2 Inhibitor. *J. Adv. Pract. Oncol.* **2022**, *13*, 158–163. [[CrossRef](#)]
69. Fujisawa, H.; Reis, R.M.; Nakamura, M.; Colella, S.; Yonekawa, Y.; Kleihues, P.; Ohgaki, H. Loss of heterozygosity on chromosome 10 is more extensive in primary (de novo) than in secondary glioblastomas. *Lab. Invest.* **2000**, *80*, 65–72. [[CrossRef](#)]
70. Balesaria, S.; Brock, C.; Bower, M.; Clark, J.; Nicholson, S.K.; Lewis, P.; de Sanctis, S.; Evans, H.; Peterson, D.; Mendoza, N.; et al. Loss of chromosome 10 is an independent prognostic factor in high-grade gliomas. *Br. J. Cancer* **1999**, *81*, 1371–1377. [[CrossRef](#)]
71. Wiles, B.; Miao, M.; Coyne, E.; Larose, L.; Cybulsky, A.V.; Wing, S.S. USP19 deubiquitinating enzyme inhibits muscle cell differentiation by suppressing unfolded-protein response signaling. *Mol. Biol. Cell* **2015**, *26*, 913–923. [[CrossRef](#)] [[PubMed](#)]
72. Harada, K.; Kato, M.; Nakamura, N. USP19-Mediated Deubiquitination Facilitates the Stabilization of HRD1 Ubiquitin Ligase. *Int. J. Mol. Sci.* **2016**, *17*, 1829. [[CrossRef](#)]
73. Nagai, A.; Kadowaki, H.; Maruyama, T.; Takeda, K.; Nishitoh, H.; Ichijo, H. USP14 inhibits ER-associated degradation via interaction with IRE1 α . *Biochem. Biophys. Res. Commun.* **2009**, *379*, 995–1000. [[CrossRef](#)] [[PubMed](#)]
74. Blount, J.R.; Burr, A.A.; Denuc, A.; Marfany, G.; Todi, S.V. Ubiquitin-specific protease 25 functions in Endoplasmic Reticulum-associated degradation. *PLoS ONE* **2012**, *7*, e36542. [[CrossRef](#)]
75. Zhu, D.; Xu, R.; Huang, X.; Tang, Z.; Tian, Y.; Zhang, J.; Zheng, X. Deubiquitinating enzyme OTUB1 promotes cancer cell immunosuppression via preventing ER-associated degradation of immune checkpoint protein PD-L1. *Cell Death Differ.* **2021**, *28*, 1773–1789. [[CrossRef](#)]
76. Wu, Q.; Huang, Y.; Gu, L.; Chang, Z.; Li, G.M. OTUB1 stabilizes mismatch repair protein MSH2 by blocking ubiquitination. *J. Biol. Chem.* **2021**, *296*, 100466. [[CrossRef](#)] [[PubMed](#)]
77. Unda, B.K.; Chalil, L.; Yoon, S.; Kilpatrick, S.; Irwin, C.; Xing, S.; Murtaza, N.; Cheng, A.; Brown, C.; Afonso, A.; et al. Impaired OTUD7A-dependent Ankyrin regulation mediates neuronal dysfunction in mouse and human models of the 15q13.3 microdeletion syndrome. *Mol. Psychiatry* **2023**, *28*, 1747–1769. [[CrossRef](#)]
78. Yin, J.; Chen, W.; Chao, E.S.; Soriano, S.; Wang, L.; Wang, W.; Cummock, S.E.; Tao, H.; Pang, K.; Liu, Z.; et al. Otud7a Knockout Mice Recapitulate Many Neurological Features of 15q13.3 Microdeletion Syndrome. *Am. J. Hum. Genet.* **2018**, *102*, 296–308. [[CrossRef](#)]
79. Bonacci, T.; Emanuele, M.J. Dissenting degradation: Deubiquitinases in cell cycle and cancer. *Semin. Cancer Biol.* **2020**, *67*, 145–158. [[CrossRef](#)]
80. Das, T.; Chen, Z.; Hendriks, R.W.; Kool, M. A20/Tumor Necrosis Factor α -Induced Protein 3 in Immune Cells Controls Development of Autoinflammation and Autoimmunity: Lessons from Mouse Models. *Front. Immunol.* **2018**, *9*, 104. [[CrossRef](#)]
81. Ando, M.; Sato, Y.; Takata, K.; Nomoto, J.; Nakamura, S.; Ohshima, K.; Takeuchi, T.; Orita, Y.; Kobayashi, Y.; Yoshino, T. A20 (TNFAIP3) deletion in Epstein-Barr virus-associated lymphoproliferative disorders/lymphomas. *PLoS ONE* **2013**, *8*, e56741. [[CrossRef](#)]
82. Malakhova, O.A.; Kim, K.I.; Luo, J.K.; Zou, W.; Kumar, K.G.; Fuchs, S.Y.; Shuai, K.; Zhang, D.E. UBP43 is a novel regulator of interferon signaling independent of its ISG15 isopeptidase activity. *EMBO J.* **2006**, *25*, 2358–2367. [[CrossRef](#)]
83. Le, J.; Perez, E.; Nemzow, L.; Gong, F. Role of deubiquitinases in DNA damage response. *DNA Repair* **2019**, *76*, 89–98. [[CrossRef](#)] [[PubMed](#)]

84. Lai, K.P.; Chen, J.; Tse, W.K.F. Role of Deubiquitinases in Human Cancers: Potential Targeted Therapy. *Int. J. Mol. Sci.* **2020**, *21*, 2548. [[CrossRef](#)] [[PubMed](#)]
85. Nakamura, N.; Hirose, S. Regulation of mitochondrial morphology by USP30, a deubiquitinating enzyme present in the mitochondrial outer membrane. *Mol. Biol. Cell* **2008**, *19*, 1903–1911. [[CrossRef](#)]
86. Wauer, T.; Swatek, K.N.; Wagstaff, J.L.; Gladkova, C.; Pruneda, J.N.; Michel, M.A.; Gersch, M.; Johnson, C.M.; Freund, S.M.; Komander, D. Ubiquitin Ser65 phosphorylation affects ubiquitin structure, chain assembly and hydrolysis. *EMBO J.* **2015**, *34*, 307–325. [[CrossRef](#)] [[PubMed](#)]
87. Cunningham, C.N.; Baughman, J.M.; Phu, L.; Tea, J.S.; Yu, C.; Coons, M.; Kirkpatrick, D.S.; Bingol, B.; Corn, J.E. USP30 and parkin homeostatically regulate atypical ubiquitin chains on mitochondria. *Nat. Cell Biol.* **2015**, *17*, 160–169. [[CrossRef](#)] [[PubMed](#)]
88. Bingol, B.; Tea, J.S.; Phu, L.; Reichelt, M.; Bakalarski, C.E.; Song, Q.; Foreman, O.; Kirkpatrick, D.S.; Sheng, M. The mitochondrial deubiquitinase USP30 opposes parkin-mediated mitophagy. *Nature* **2014**, *510*, 370–375. [[CrossRef](#)]
89. Sato, Y.; Yoshikawa, A.; Yamagata, A.; Mimura, H.; Yamashita, M.; Ookata, K.; Nureki, O.; Iwai, K.; Komada, M.; Fukai, S. Structural basis for specific cleavage of Lys 63-linked polyubiquitin chains. *Nature* **2008**, *455*, 358–362. [[CrossRef](#)]
90. Wang, D.; Xu, C.; Yang, W.; Chen, J.; Ou, Y.; Guan, Y.; Guan, J.; Liu, Y. E3 ligase RNF167 and deubiquitinase STAMBPL1 modulate mTOR and cancer progression. *Mol. Cell* **2022**, *82*, 770–784.e9. [[CrossRef](#)]
91. Mahul-Mellier, A.L.; Pazarentzos, E.; Datler, C.; Iwasawa, R.; AbuAli, G.; Lin, B.; Grimm, S. De-ubiquitinating protease USP2a targets RIP1 and TRAF2 to mediate cell death by TNF. *Cell Death Differ.* **2012**, *19*, 891–899. [[CrossRef](#)]
92. Xu, G.; Tan, X.; Wang, H.; Sun, W.; Shi, Y.; Burlingame, S.; Gu, X.; Cao, G.; Zhang, T.; Qin, J.; et al. Ubiquitin-specific peptidase 21 inhibits tumor necrosis factor α -induced nuclear factor κ B activation via binding to and deubiquitinating receptor-interacting protein 1. *J. Biol. Chem.* **2010**, *285*, 969–978. [[CrossRef](#)]
93. Gorick, F.; Vu, V.; Smith, L.; Scheib, U.; Bohm, R.; Akkili, N.; Wohlfahrt, G.; Weiske, J.; Bomer, U.; Brzezinka, K.; et al. Discovery and Characterization of BAY-805, a Potent and Selective Inhibitor of Ubiquitin-Specific Protease USP21. *J. Med. Chem.* **2023**, *66*, 3431–3447. [[CrossRef](#)] [[PubMed](#)]
94. Pajtler, K.W.; Mack, S.C.; Ramaswamy, V.; Smith, C.A.; Witt, H.; Smith, A.; Hansford, J.R.; von Hoff, K.; Wright, K.D.; Hwang, E.; et al. The current consensus on the clinical management of intracranial ependymoma and its distinct molecular variants. *Acta Neuropathol.* **2017**, *133*, 5–12. [[CrossRef](#)] [[PubMed](#)]
95. Hyrskyluoto, A.; Bruelle, C.; Lundh, S.H.; Do, H.T.; Kivinen, J.; Rappou, E.; Reijonen, S.; Waltimo, T.; Petersen, A.; Lindholm, D.; et al. Ubiquitin-specific protease-14 reduces cellular aggregates and protects against mutant huntingtin-induced cell degeneration: Involvement of the proteasome and ER stress-activated kinase IRE1 α . *Hum. Mol. Genet.* **2014**, *23*, 5928–5939. [[CrossRef](#)]
96. Giordano, M.; Roncagalli, R.; Bourdely, P.; Chasson, L.; Buferne, M.; Yamasaki, S.; Beyaert, R.; van Loo, G.; Auphan-Anezin, N.; Schmitt-Verhulst, A.M.; et al. The tumor necrosis factor alpha-induced protein 3 (TNFAIP3, A20) imposes a brake on antitumor activity of CD8 T cells. *Proc. Natl. Acad. Sci. USA* **2014**, *111*, 11115–11120. [[CrossRef](#)] [[PubMed](#)]
97. Momtazi, G.; Lambrecht, B.N.; Naranjo, J.R.; Schock, B.C. Regulators of A20 (TNFAIP3): New drug-able targets in inflammation. *Am. J. Physiol. Lung Cell. Mol. Physiol.* **2019**, *316*, L456–L469. [[CrossRef](#)]
98. van Bon, B.W.M.; Mefford, H.C.; de Vries, B.B.A.; Schaaf, C.P. 15q13.3 Recurrent Deletion. In *GeneReviews*(*R*); Adam, M.P., Mirzaa, G.M., Pagon, R.A., Wallace, S.E., Bean, L.J.H., Gripp, K.W., Amemiya, A., Eds.; University of Washington: Seattle, WA, USA, 1993.
99. Uddin, M.; Unda, B.K.; Kwan, V.; Holzapfel, N.T.; White, S.H.; Chalil, L.; Woodbury-Smith, M.; Ho, K.S.; Harward, E.; Murtaza, N.; et al. OTUD7A Regulates Neurodevelopmental Phenotypes in the 15q13.3 Microdeletion Syndrome. *Am. J. Hum. Genet.* **2018**, *102*, 278–295. [[CrossRef](#)] [[PubMed](#)]
100. Lim, J.H.; Ha, U.H.; Woo, C.H.; Xu, H.; Li, J.D. CYLD is a crucial negative regulator of innate immune response in Escherichia coli pneumonia. *Cell. Microbiol.* **2008**, *10*, 2247–2256. [[CrossRef](#)]
101. Deng, M.; Dai, W.; Yu, V.Z.; Tao, L.; Lung, M.L. Cylindromatosis Lysine 63 Deubiquitinase (CYLD) Regulates NF- κ B Signaling Pathway and Modulates Fibroblast and Endothelial Cells Recruitment in Nasopharyngeal Carcinoma. *Cancers* **2020**, *12*, 1924. [[CrossRef](#)]
102. Sun, S.C. CYLD: A tumor suppressor deubiquitinase regulating NF- κ B activation and diverse biological processes. *Cell Death Differ.* **2010**, *17*, 25–34. [[CrossRef](#)] [[PubMed](#)]
103. Stevenson, L.F.; Sparks, A.; Allende-Vega, N.; Xirodimas, D.P.; Lane, D.P.; Saville, M.K. The deubiquitinating enzyme USP2a regulates the p53 pathway by targeting Mdm2. *EMBO J.* **2007**, *26*, 976–986. [[CrossRef](#)] [[PubMed](#)]
104. Shan, J.; Zhao, W.; Gu, W. Suppression of cancer cell growth by promoting cyclin D1 degradation. *Mol. Cell* **2009**, *36*, 469–476. [[CrossRef](#)] [[PubMed](#)]
105. Yang, Y.; Duguay, D.; Fahrenkrug, J.; Cermakian, N.; Wing, S.S. USP2 regulates the intracellular localization of PER1 and circadian gene expression. *J. Biol. Rhythm.* **2014**, *29*, 243–256. [[CrossRef](#)] [[PubMed](#)]
106. Scoma, H.D.; Humby, M.; Yadav, G.; Zhang, Q.; Fogerty, J.; Besharse, J.C. The de-ubiquitylating enzyme, USP2, is associated with the circadian clockwork and regulates its sensitivity to light. *PLoS ONE* **2011**, *6*, e25382. [[CrossRef](#)]
107. Stojkovic, K.; Wing, S.S.; Cermakian, N. A central role for ubiquitination within a circadian clock protein modification code. *Front. Mol. Neurosci.* **2014**, *7*, 69. [[CrossRef](#)]
108. He, J.; Lee, H.J.; Saha, S.; Ruan, D.; Guo, H.; Chan, C.H. Inhibition of USP2 eliminates cancer stem cells and enhances TNBC responsiveness to chemotherapy. *Cell Death Dis.* **2019**, *10*, 285. [[CrossRef](#)]

109. Xiao, W.; Wang, J.; Wang, X.; Cai, S.; Guo, Y.; Ye, L.; Li, D.; Hu, A.; Jin, S.; Yuan, B.; et al. Therapeutic targeting of the USP2-E2F4 axis inhibits autophagic machinery essential for zinc homeostasis in cancer progression. *Autophagy* **2022**, *18*, 2615–2635. [[CrossRef](#)]
110. Lee, J.H.; Zou, L.; Yang, R.; Han, J.; Wan, Q.; Zhang, X.; El Baghdady, S.; Roman, A.; Elly, C.; Jin, H.S.; et al. The deubiquitinase CYLD controls protective immunity against helminth infection by regulation of Treg cell plasticity. *J. Allergy Clin. Immunol.* **2021**, *148*, 209–224.e9. [[CrossRef](#)]
111. Bustamante, H.A.; Cereceda, K.; Gonzalez, A.E.; Valenzuela, G.E.; Cheuquemilla, Y.; Hernandez, S.; Arias-Munoz, E.; Cerda-Troncoso, C.; Bandau, S.; Soza, A.; et al. The Proteasomal Deubiquitinating Enzyme PSMD14 Regulates Macroautophagy by Controlling Golgi-to-ER Retrograde Transport. *Cells* **2020**, *9*, 777. [[CrossRef](#)]
112. Bustamante, H.A.; Albornoz, N.; Morselli, E.; Soza, A.; Burgos, P.V. Novel insights into the non-canonical roles of PSMD14/POH1/Rpn11 in proteostasis and in the modulation of cancer progression. *Cell. Signal.* **2023**, *101*, 110490. [[CrossRef](#)]
113. Zhang, D.; Zaugg, K.; Mak, T.W.; Elledge, S.J. A role for the deubiquitinating enzyme USP28 in control of the DNA-damage response. *Cell* **2006**, *126*, 529–542. [[CrossRef](#)]
114. Jacq, X.; Kemp, M.; Martin, N.M.; Jackson, S.P. Deubiquitylating enzymes and DNA damage response pathways. *Cell Biochem. Biophys.* **2013**, *67*, 25–43. [[CrossRef](#)]
115. Liang, X.W.; Wang, S.Z.; Liu, B.; Chen, J.C.; Cao, Z.; Chu, F.R.; Lin, X.; Liu, H.; Wu, J.C. A review of deubiquitinases and their roles in tumorigenesis and development. *Front. Bioeng. Biotechnol.* **2023**, *11*, 1204472. [[CrossRef](#)]
116. Huo, Y.; Khatri, N.; Hou, Q.; Gilbert, J.; Wang, G.; Man, H.Y. The deubiquitinating enzyme USP46 regulates AMPA receptor ubiquitination and trafficking. *J. Neurochem.* **2015**, *134*, 1067–1080. [[CrossRef](#)] [[PubMed](#)]
117. Anggono, V.; Haganir, R.L. Regulation of AMPA receptor trafficking and synaptic plasticity. *Curr. Opin. Neurobiol.* **2012**, *22*, 461–469. [[CrossRef](#)] [[PubMed](#)]
118. Ishiuchi, S.; Tsuzuki, K.; Yoshida, Y.; Yamada, N.; Hagimura, N.; Okado, H.; Miwa, A.; Kurihara, H.; Nakazato, Y.; Tamura, M.; et al. Blockage of Ca(2+)-permeable AMPA receptors suppresses migration and induces apoptosis in human glioblastoma cells. *Nat. Med.* **2002**, *8*, 971–978. [[CrossRef](#)] [[PubMed](#)]
119. Piao, Y.; Lu, L.; de Groot, J. AMPA receptors promote perivascular glioma invasion via β 1 integrin-dependent adhesion to the extracellular matrix. *Neuro. Oncol.* **2009**, *11*, 260–273. [[CrossRef](#)]
120. Krishna, S.; Choudhury, A.; Keough, M.B.; Seo, K.; Ni, L.; Kakaizada, S.; Lee, A.; Aabedi, A.; Popova, G.; Lipkin, B.; et al. Glioblastoma remodelling of human neural circuits decreases survival. *Nature* **2023**, *617*, 599–607. [[CrossRef](#)]
121. Tomida, S.; Mamiya, T.; Sakamaki, H.; Miura, M.; Aosaki, T.; Masuda, M.; Niwa, M.; Kameyama, T.; Kobayashi, J.; Iwaki, Y.; et al. Usp46 is a quantitative trait gene regulating mouse immobile behavior in the tail suspension and forced swimming tests. *Nat. Genet.* **2009**, *41*, 688–695. [[CrossRef](#)]
122. Xian, J.; Zhang, Q.; Guo, X.; Liang, X.; Liu, X.; Feng, Y. A prognostic signature based on three non-coding RNAs for prediction of the overall survival of glioma patients. *FEBS Open Bio.* **2019**, *9*, 682–692. [[CrossRef](#)] [[PubMed](#)]
123. Smits, A.; Jin, Z.; Elsir, T.; Pedder, H.; Nister, M.; Alafuzoff, I.; Dimberg, A.; Edqvist, P.H.; Ponten, F.; Aronica, E.; et al. GABA-A channel subunit expression in human glioma correlates with tumor histology and clinical outcome. *PLoS ONE* **2012**, *7*, e37041. [[CrossRef](#)] [[PubMed](#)]
124. Blanchart, A.; Fernando, R.; Haring, M.; Assaife-Lopes, N.; Romanov, R.A.; Andang, M.; Harkany, T.; Ernfor, P. Endogenous GAB(AA) receptor activity suppresses glioma growth. *Oncogene* **2017**, *36*, 777–786. [[CrossRef](#)] [[PubMed](#)]
125. Ma, L.; Lin, K.; Chang, G.; Chen, Y.; Yue, C.; Guo, Q.; Zhang, S.; Jia, Z.; Huang, T.T.; Zhou, A.; et al. Aberrant Activation of β -Catenin Signaling Drives Glioma Tumorigenesis via USP1-Mediated Stabilization of EZH2. *Cancer Res.* **2019**, *79*, 72–85. [[CrossRef](#)]
126. Li, Z.; Li, M.; Wang, D.; Hou, P.; Chen, X.; Chu, S.; Chai, D.; Zheng, J.; Bai, J. Post-translational modifications of EZH2 in cancer. *Cell Biosci.* **2020**, *10*, 143. [[CrossRef](#)]
127. Nibe, Y.; Oshima, S.; Kobayashi, M.; Maeyashiki, C.; Matsuzawa, Y.; Otsubo, K.; Matsuda, H.; Aonuma, E.; Nemoto, Y.; Nagaishi, T.; et al. Novel polyubiquitin imaging system, PolyUb-FC, reveals that K33-linked polyubiquitin is recruited by SQSTM1/p62. *Autophagy* **2018**, *14*, 347–358. [[CrossRef](#)]
128. Chen, Y.H.; Chen, H.H.; Wang, W.J.; Chen, H.Y.; Huang, W.S.; Kao, C.H.; Lee, S.R.; Yeat, N.Y.; Yan, R.L.; Chan, S.J.; et al. TRABID inhibition activates cGAS/STING-mediated anti-tumor immunity through mitosis and autophagy dysregulation. *Nat. Commun.* **2023**, *14*, 3050. [[CrossRef](#)]
129. Afonina, I.S.; Beyaert, R. Trabid epigenetically drives expression of IL-12 and IL-23. *Nat. Immunol.* **2016**, *17*, 227–228. [[CrossRef](#)]
130. Jin, J.; Xie, X.; Xiao, Y.; Hu, H.; Zou, Q.; Cheng, X.; Sun, S.C. Epigenetic regulation of the expression of IL12 and IL23 and autoimmune inflammation by the deubiquitinase Trabid. *Nat. Immunol.* **2016**, *17*, 259–268. [[CrossRef](#)]
131. Ma, J.; Zhou, Y.; Pan, P.; Yu, H.; Wang, Z.; Li, L.L.; Wang, B.; Yan, Y.; Pan, Y.; Ye, Q.; et al. TRABID overexpression enables synthetic lethality to PARP inhibitor via prolonging 53BP1 retention at double-strand breaks. *Nat. Commun.* **2023**, *14*, 1810. [[CrossRef](#)]
132. Wertz, I.E.; O'Rourke, K.M.; Zhou, H.; Eby, M.; Aravind, L.; Seshagiri, S.; Wu, P.; Wiesmann, C.; Baker, R.; Boone, D.L.; et al. De-ubiquitination and ubiquitin ligase domains of A20 downregulate NF- κ B signalling. *Nature* **2004**, *430*, 694–699. [[CrossRef](#)] [[PubMed](#)]
133. Wertz, I.E.; Newton, K.; Seshasayee, D.; Kusam, S.; Lam, C.; Zhang, J.; Popovych, N.; Helgason, E.; Schoeffler, A.; Jeet, S.; et al. Phosphorylation and linear ubiquitin direct A20 inhibition of inflammation. *Nature* **2015**, *528*, 370–375. [[CrossRef](#)] [[PubMed](#)]

134. Abbasi, A.; Forsberg, K.; Bischof, F. The role of the ubiquitin-editing enzyme A20 in diseases of the central nervous system and other pathological processes. *Front. Mol. Neurosci.* **2015**, *8*, 21. [[CrossRef](#)] [[PubMed](#)]
135. Catrysse, L.; Vereecke, L.; Beyaert, R.; van Loo, G. A20 in inflammation and autoimmunity. *Trends Immunol.* **2014**, *35*, 22–31. [[CrossRef](#)]
136. Opirari, A.W., Jr.; Boguski, M.S.; Dixit, V.M. The A20 cDNA induced by tumor necrosis factor alpha encodes a novel type of zinc finger protein. *J. Biol. Chem.* **1990**, *265*, 14705–14708. [[CrossRef](#)]
137. Bredel, M.; Bredel, C.; Juric, D.; Duran, G.E.; Yu, R.X.; Harsh, G.R.; Vogel, H.; Recht, L.D.; Scheck, A.C.; Sikic, B.I. Tumor necrosis factor-alpha-induced protein 3 as a putative regulator of nuclear factor- κ B-mediated resistance to O6-alkylating agents in human glioblastomas. *J. Clin. Oncol.* **2006**, *24*, 274–287. [[CrossRef](#)]
138. Hjelmeland, A.B.; Wu, Q.; Wickman, S.; Eyler, C.; Heddeleston, J.; Shi, Q.; Lathia, J.D.; Macswords, J.; Lee, J.; McLendon, R.E.; et al. Targeting A20 decreases glioma stem cell survival and tumor growth. *PLoS Biol.* **2010**, *8*, e1000319. [[CrossRef](#)]
139. Sharma, T.; Schwalbe, E.C.; Williamson, D.; Sill, M.; Hovestadt, V.; Mynarek, M.; Rutkowski, S.; Robinson, G.W.; Gajjar, A.; Cavalli, F.; et al. Second-generation molecular subgrouping of medulloblastoma: An international meta-analysis of Group 3 and Group 4 subtypes. *Acta Neuropathol.* **2019**, *138*, 309–326. [[CrossRef](#)]
140. Jung, M.; Russell, A.J.; Liu, B.; George, J.; Liu, P.Y.; Liu, T.; DeFazio, A.; Bowtell, D.D.; Oberthuer, A.; London, W.B.; et al. A Myc Activity Signature Predicts Poor Clinical Outcomes in Myc-Associated Cancers. *Cancer Res.* **2017**, *77*, 971–981. [[CrossRef](#)]
141. Kitamura, H.; Hashimoto, M. USP2-Related Cellular Signaling and Consequent Pathophysiological Outcomes. *Int. J. Mol. Sci.* **2021**, *22*, 1209. [[CrossRef](#)]
142. Benassi, B.; Flavin, R.; Marchionni, L.; Zanata, S.; Pan, Y.; Chowdhury, D.; Marani, M.; Strano, S.; Muti, P.; Blandino, G.; et al. MYC is activated by USP2a-mediated modulation of microRNAs in prostate cancer. *Cancer Discov.* **2012**, *2*, 236–247. [[CrossRef](#)]
143. Petrosyan, E.; Fares, J.; Fernandez, L.G.; Yeeravalli, R.; Dmello, C.; Duffy, J.T.; Zhang, P.; Lee-Chang, C.; Miska, J.; Ahmed, A.U.; et al. Endoplasmic Reticulum Stress in the Brain Tumor Immune Microenvironment. *Mol. Cancer Res.* **2023**, *21*, 389–396. [[CrossRef](#)] [[PubMed](#)]
144. Mitchell, D.; Shireman, J.; Sierra Potchanant, E.A.; Lara-Velazquez, M.; Dey, M. Neuroinflammation in Autoimmune Disease and Primary Brain Tumors: The Quest for Striking the Right Balance. *Front. Cell. Neurosci.* **2021**, *15*, 716947. [[CrossRef](#)] [[PubMed](#)]
145. Pelizzari-Raymundo, D.; Doultinos, D.; Pineau, R.; Sauzay, C.; Koutsandreas, T.; Langlais, T.; Carlesso, A.; Gkotsi, E.; Negroni, L.; Avril, T.; et al. A novel IRE1 kinase inhibitor for adjuvant glioblastoma treatment. *iScience* **2023**, *26*, 106687. [[CrossRef](#)] [[PubMed](#)]
146. Flores-Santibanez, F.; Rennen, S.; Fernandez, D.; De Nolf, C.; Van De Velde, E.; Gaete Gonzalez, S.; Fuentes, C.; Moreno, C.; Figueroa, D.; Lladser, A.; et al. Nuanced role for dendritic cell intrinsic IRE1 RNase in the regulation of antitumor adaptive immunity. *Front. Immunol.* **2023**, *14*, 1209588. [[CrossRef](#)]
147. Liang, W.; Fang, J.; Zhou, S.; Hu, W.; Yang, Z.; Li, Z.; Dai, L.; Tao, Y.; Fu, X.; Wang, X. The role of ubiquitin-specific peptidases in glioma progression. *Biomed. Pharmacother.* **2022**, *146*, 112585. [[CrossRef](#)]
148. Hanna, J.; Hathaway, N.A.; Tone, Y.; Crosas, B.; Elsasser, S.; Kirkpatrick, D.S.; Leggett, D.S.; Gygi, S.P.; King, R.W.; Finley, D. Deubiquitinating enzyme Ubp6 functions noncatalytically to delay proteasomal degradation. *Cell* **2006**, *127*, 99–111. [[CrossRef](#)]
149. Lee, B.H.; Lee, M.J.; Park, S.; Oh, D.C.; Elsasser, S.; Chen, P.C.; Gartner, C.; Dimova, N.; Hanna, J.; Gygi, S.P.; et al. Enhancement of proteasome activity by a small-molecule inhibitor of USP14. *Nature* **2010**, *467*, 179–184. [[CrossRef](#)]
150. Lee, J.H.; Shin, S.K.; Jiang, Y.; Choi, W.H.; Hong, C.; Kim, D.E.; Lee, M.J. Facilitated Tau Degradation by USP14 Aptamers via Enhanced Proteasome Activity. *Sci. Rep.* **2015**, *5*, 10757. [[CrossRef](#)]
151. Zhu, Y.; Zhang, C.; Gu, C.; Li, Q.; Wu, N. Function of Deubiquitinating Enzyme USP14 as Oncogene in Different Types of Cancer. *Cell. Physiol. Biochem.* **2016**, *38*, 993–1002. [[CrossRef](#)]
152. Ma, Y.S.; Wang, X.F.; Zhang, Y.J.; Luo, P.; Long, H.D.; Li, L.; Yang, H.Q.; Xie, R.T.; Jia, C.Y.; Lu, G.X.; et al. Inhibition of USP14 Deubiquitinating Activity as a Potential Therapy for Tumors with p53 Deficiency. *Mol. Ther. Oncolytics* **2020**, *16*, 147–157. [[CrossRef](#)] [[PubMed](#)]
153. Kaokhum, N.; Pinto-Fernandez, A.; Wilkinson, M.; Kessler, B.M.; Ismail, H.M. The Mechano-Ubiquitinome of Articular Cartilage: Differential Ubiquitination and Activation of a Group of ER-Associated DUBs and ER Stress Regulators. *Mol. Cell. Proteom.* **2022**, *21*, 100419. [[CrossRef](#)]
154. Ernst, R.; Mueller, B.; Ploegh, H.L.; Schlieker, C. The otubain YOD1 is a deubiquitinating enzyme that associates with p97 to facilitate protein dislocation from the ER. *Mol. Cell* **2009**, *36*, 28–38. [[CrossRef](#)] [[PubMed](#)]
155. Schimmack, G.; Schorpp, K.; Kutzner, K.; Gehring, T.; Brenke, J.K.; Hadian, K.; Krappmann, D. YOD1/TRAF6 association balances p62-dependent IL-1 signaling to NF- κ B. *Elife* **2017**, *6*, e22416. [[CrossRef](#)]
156. Tanji, K.; Mori, F.; Miki, Y.; Utsumi, J.; Sasaki, H.; Kakita, A.; Takahashi, H.; Wakabayashi, K. YOD1 attenuates neurogenic proteotoxicity through its deubiquitinating activity. *Neurobiol. Dis.* **2018**, *112*, 14–23. [[CrossRef](#)]
157. Zhou, L.; Li, L.; Chen, Y.; Chen, C.; Zhi, Z.; Yan, L.; Wang, Y.; Liu, B.; Zhai, Q. miR-190a-3p Promotes Proliferation and Migration in Glioma Cells via YOD1. *Comput. Math. Methods Med.* **2021**, *2021*, 3957738. [[CrossRef](#)] [[PubMed](#)]
158. Kim, Y.; Kim, W.; Song, Y.; Kim, J.R.; Cho, K.; Moon, H.; Ro, S.W.; Seo, E.; Ryu, Y.M.; Myung, S.J.; et al. Deubiquitinase YOD1 potentiates YAP/TAZ activities through enhancing ITCH stability. *Proc. Natl. Acad. Sci. USA* **2017**, *114*, 4691–4696. [[CrossRef](#)] [[PubMed](#)]
159. Masliantsev, K.; Karayan-Tapon, L.; Guichet, P.O. Hippo Signaling Pathway in Gliomas. *Cells* **2021**, *10*, 184. [[CrossRef](#)]

160. Nijman, S.M.; Huang, T.T.; Dirac, A.M.; Brummelkamp, T.R.; Kerkhoven, R.M.; D'Andrea, A.D.; Bernards, R. The deubiquitinating enzyme USP1 regulates the Fanconi anemia pathway. *Mol. Cell* **2005**, *17*, 331–339. [[CrossRef](#)]
161. Huang, T.T.; Nijman, S.M.; Mirchandani, K.D.; Galardy, P.J.; Cohn, M.A.; Haas, W.; Gygi, S.P.; Ploegh, H.L.; Bernards, R.; D'Andrea, A.D. Regulation of monoubiquitinated PCNA by DUB autocleavage. *Nat. Cell Biol.* **2006**, *8*, 339–347. [[CrossRef](#)]
162. Kashiwaba, S.; Kanao, R.; Masuda, Y.; Kusumoto-Matsuo, R.; Hanaoka, F.; Masutani, C. USP7 Is a Suppressor of PCNA Ubiquitination and Oxidative-Stress-Induced Mutagenesis in Human Cells. *Cell Rep.* **2015**, *13*, 2072–2080. [[CrossRef](#)] [[PubMed](#)]
163. Parsons, J.L.; Dianova, I.I.; Khoronenkova, S.V.; Edelmann, M.J.; Kessler, B.M.; Dianov, G.L. USP47 is a deubiquitylating enzyme that regulates base excision repair by controlling steady-state levels of DNA polymerase β . *Mol. Cell* **2011**, *41*, 609–615. [[CrossRef](#)] [[PubMed](#)]
164. Zhao, Y.; Majid, M.C.; Soll, J.M.; Brickner, J.R.; Dango, S.; Mosammamarast, N. Noncanonical regulation of alkylation damage resistance by the OTUD4 deubiquitinase. *EMBO J.* **2015**, *34*, 1687–1703. [[CrossRef](#)]
165. Chitale, S.; Richly, H. Timing of DNA lesion recognition: Ubiquitin signaling in the NER pathway. *Cell Cycle* **2017**, *16*, 163–171. [[CrossRef](#)]
166. Perez-Oliva, A.B.; Lachaud, C.; Szyniarowski, P.; Munoz, I.; Macartney, T.; Hickson, I.; Rouse, J.; Alessi, D.R. USP45 deubiquitylase controls ERCC1-XPF endonuclease-mediated DNA damage responses. *EMBO J.* **2015**, *34*, 326–343. [[CrossRef](#)]
167. Nishi, R.; Wijnhoven, P.; le Sage, C.; Tjeertes, J.; Galanty, Y.; Forment, J.V.; Clague, M.J.; Urbe, S.; Jackson, S.P. Systematic characterization of deubiquitylating enzymes for roles in maintaining genome integrity. *Nat. Cell Biol.* **2014**, *16*, 1016–1026. [[CrossRef](#)]
168. Sato, Y.; Yamagata, A.; Goto-Ito, S.; Kubota, K.; Miyamoto, R.; Nakada, S.; Fukai, S. Molecular basis of Lys-63-linked polyubiquitination inhibition by the interaction between human deubiquitinating enzyme OTUB1 and ubiquitin-conjugating enzyme UBC13. *J. Biol. Chem.* **2012**, *287*, 25860–25868. [[CrossRef](#)] [[PubMed](#)]
169. Butler, L.R.; Densham, R.M.; Jia, J.; Garvin, A.J.; Stone, H.R.; Shah, V.; Weekes, D.; Festy, F.; Beesley, J.; Morris, J.R. The proteasomal de-ubiquitinating enzyme POH1 promotes the double-strand DNA break response. *EMBO J.* **2012**, *31*, 3918–3934. [[CrossRef](#)]
170. Kakarougkas, A.; Ismail, A.; Katsuki, Y.; Freire, R.; Shibata, A.; Jeggo, P.A. Co-operation of BRCA1 and POH1 relieves the barriers posed by 53BP1 and RAP80 to resection. *Nucleic Acids Res.* **2013**, *41*, 10298–10311. [[CrossRef](#)]
171. Vincent, P.; Collette, Y.; Marignier, R.; Vuailat, C.; Rogemond, V.; Davoust, N.; Malcus, C.; Cavagna, S.; Gessain, A.; Machuca-Gayet, I.; et al. A role for the neuronal protein collapsin response mediator protein 2 in T lymphocyte polarization and migration. *J. Immunol.* **2005**, *175*, 7650–7660. [[CrossRef](#)]
172. Nakamura, F.; Ohshima, T.; Goshima, Y. Collapsin Response Mediator Proteins: Their Biological Functions and Pathophysiology in Neuronal Development and Regeneration. *Front. Cell. Neurosci.* **2020**, *14*, 188. [[CrossRef](#)]
173. Bedekovics, T.; Hussain, S.; Zhang, Y.; Ali, A.; Jeon, Y.J.; Galardy, P.J. USP24 Is a Cancer-Associated Ubiquitin Hydrolase, Novel Tumor Suppressor, and Chromosome Instability Gene Deleted in Neuroblastoma. *Cancer Res.* **2021**, *81*, 1321–1331. [[CrossRef](#)] [[PubMed](#)]
174. Thayer, J.A.; Awad, O.; Hegdekar, N.; Sarkar, C.; Tesfay, H.; Burt, C.; Zeng, X.; Feldman, R.A.; Lipinski, M.M. The PARK10 gene USP24 is a negative regulator of autophagy and ULK1 protein stability. *Autophagy* **2020**, *16*, 140–153. [[CrossRef](#)] [[PubMed](#)]
175. Ma, X.; Qi, W.; Yang, F.; Pan, H. Deubiquitinase JOSD1 promotes tumor progression via stabilizing Snail in lung adenocarcinoma. *Am. J. Cancer Res.* **2022**, *12*, 2323–2336.
176. Yang, J.; Weisberg, E.L.; Liu, X.; Magin, R.S.; Chan, W.C.; Hu, B.; Schauer, N.J.; Zhang, S.; Lamberto, I.; Doherty, L.; et al. Small molecule inhibition of deubiquitinating enzyme JOSD1 as a novel targeted therapy for leukemias with mutant JAK2. *Leukemia* **2022**, *36*, 210–220. [[CrossRef](#)]
177. Wang, X.; Zhang, L.; Zhang, Y.; Zhao, P.; Qian, L.; Yuan, Y.; Liu, J.; Cheng, Q.; Xu, W.; Zuo, Y.; et al. JOSD1 Negatively Regulates Type-I Interferon Antiviral Activity by Deubiquitinating and Stabilizing SOCS1. *Viral Immunol.* **2017**, *30*, 342–349. [[CrossRef](#)] [[PubMed](#)]
178. Luo, Y.; Zhou, J.; Tang, J.; Zhou, F.; He, Z.; Liu, T.; Liu, T. MINDY1 promotes bladder cancer progression by stabilizing YAP. *Cancer Cell Int.* **2021**, *21*, 395. [[CrossRef](#)]
179. Tang, J.; Luo, Y.; Long, G.; Zhou, L. MINDY1 promotes breast cancer cell proliferation by stabilizing estrogen receptor α . *Cell Death Dis.* **2021**, *12*, 937. [[CrossRef](#)] [[PubMed](#)]

Disclaimer/Publisher's Note: The statements, opinions and data contained in all publications are solely those of the individual author(s) and contributor(s) and not of MDPI and/or the editor(s). MDPI and/or the editor(s) disclaim responsibility for any injury to people or property resulting from any ideas, methods, instructions or products referred to in the content.